UCRL-53286
Distribution Category UC-70

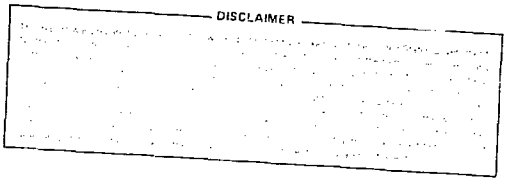

Engineering Test Plan for Field Radionuclide Migration Experiments in Climax Granite

D. Isherwood, E. Raber, R. Stone,

D. Lord, N. Rector, and R. Failor

Manuscript date: May 1, 1982

LAWRENCE LIVERMORE LABORATORY
University of California • Livermore, California • 94550

Available from: National Technical Information Service • U.S. Department of Commerce
5285 Port Royal Road • Springfield, VA 22161 • $8.00 per copy • (Microfiche $3.50)

CONTENTS

LIST OF FIGURES

LIST OF TABLES

ABSTRACT

This Engineering Test Plan (ETP) describes field studies of radionuclide migration in fractured rock designed for the Climax granite at the Nevada Test Site. The purpose of the ETP is to provide a detailed written document of the method of accomplishing these studies. The ETP contains the experimental test plans, an instrumentation plan, system schematics, a description of the test facility, and a brief outline of the laboratory support studies needed to understand the chemistry of the rock/water/radionuclide interactions. Results of our initial hydrologic investigations are presented along with pretest predictions based on the hydrologic test results.

1. INTRODUCTION

This Engineering Test Plan describes the radionuclide migration studies we plan to conduct in the Climax granite at the Nevada Test Site (NTS). The purpose of the Engineering Test Plan is to provide a detailed written document of the method of accomplishing the field test. It is intended to compliment the Program Plan [Isherwood et al. (1980)] rather than replace it. The Program Plan contains the management plan, work breakdown structure, and a general description of activities. The Engineering Test Plan contains detailed experimental test plans, an instrumentation plan, system schematics, and a description of the test facility. Results of our hydrological investigations are presented along with pretest predictions based on those preliminary results. The quality assurance (QA) and system safety aspects of this project are briefly described, since both are covered in detail in other documents. A schedule and cost plan are not included in this document since funds for this project are no longer available because of a change in funding priorities in the National Waste Terminal Storage (NWTS) program. If and when this project restarts, a revised Program Plan will be issued.

Field tests of the type described in this plan are needed to develop measurement techniques that can be used for in situ testing at candidate sites, to provide experimental data for model development and verification required for long-term risk assessment, and to determine whether laboratory

studies are sufficient to describe field conditions. This experimental basis for risk assessment of a nuclear waste repository is an important part of the NWTS Program Plan.

Our approach combines an interactive system of field and laboratory measurements of radionuclide transport and sorption in fractured rock with the use of existing hydrologic models for pretest predictions and data interpretation. This project will provide state-of-the-art field measurement techniques for radionuclide migration studies, field test data on radionuclide migration, and a comparison of field and laboratory measured retardation factors. The field test data will be available to the Waste Isolation Performance Assessment Program (WIPAP) for the verification of mass transport models designed to describe radionuclide release scenarios and their consequences.

2. TEST OBJECTIVES

Tests described in the Engineering Test Plan are designed to meet the following objectives:

- To develop equipment and procedures for a reliable field migration test that can be used at candidate repository sites in fractured rock.
- To determine field retardation factors for selected radionuclides that can be compared to laboratory measured values.
- To provide input to mass transport models that will improve our ability to make dependable pretest predictions and aid in data interpretation.

These objectives will be considered met when we have completed a migration test using both sorptive and nonsorptive radionuclides. Successful test completion is defined as that time when a sufficient number of samples are collected and analyzed to determine the shape of the concentration vs time curves and the data are analyzed using an appropriate mass transport model to determine the retardation characteristics of the injected radionuclides that have appeared at the outlet hole. Depending on the time and funding available after the completion of the first test, additional tests will be conducted on other fractures. This will allow us to determine fracture to fracture variability and further demonstrate the capability of hydrologic models to predict breakthrough times and concentration profiles based on the fracture flow characteristics. After each tracer test, rock samples containing the fracture will be obtained in the postcoring phase and analyzed (see Sec. 3.1).

3. TEST DESCRIPTION

3.1. EXPERIMENTAL CONCEPT

The experimental concept uses two boreholes drilled horizontally into the drift wall to intersect sets of vertical fractures at near right angles (Fig. 1). The boreholes are located one above the other about 2 m apart. The critical parts of the experiment are to successfully isolate an individual fracture between the boreholes and to establish flow along that fracture so that most of the fluid injected into the top hole is recovered from the bottom hole.

Boreholes are drilled to intersect one of the major fracture sets (see Sec. 3.3). The cores are logged and returned to LLNL for use in the laboratory studies. Each borehole is visually logged using a high-quality optical borescope with a 35-mm camera attachment for photodocumentation. The scope is scribed at measured intervals to accurately determine the fracture location within the borehole. Fractures are selected for testing that are at least one tunnel diameter away from the drift wall (i.e., more than 3 m) to avoid the fractures induced by mining. Section 4.1 describes the hydraulic test procedure used to locate suitable fractures for the migration experiments. The use of the borescope to show that a flow path exists between the upper and lower boreholes is explained in Sec. 5.6.

The migration experiments will be conducted in two phases. The first will be a series of injections of radionuclide solutions into the fracture followed by sample collection and analysis. The second will be a postmortem test analysis of the fracture material between the inlet and outlet hole that has been recovered by back-coring into the fracture at the completion of the migration experiments.

The following outlines the planned sequence of events in the experimental procedure after a suitable fracture has been chosen and pretest predictions based on the hydraulic tests have been made:

1. A steady-state flow will be established along the fracture using either natural granitic ground water or a synthetic ground water, based on the chemical analyses of the Climax ground water.

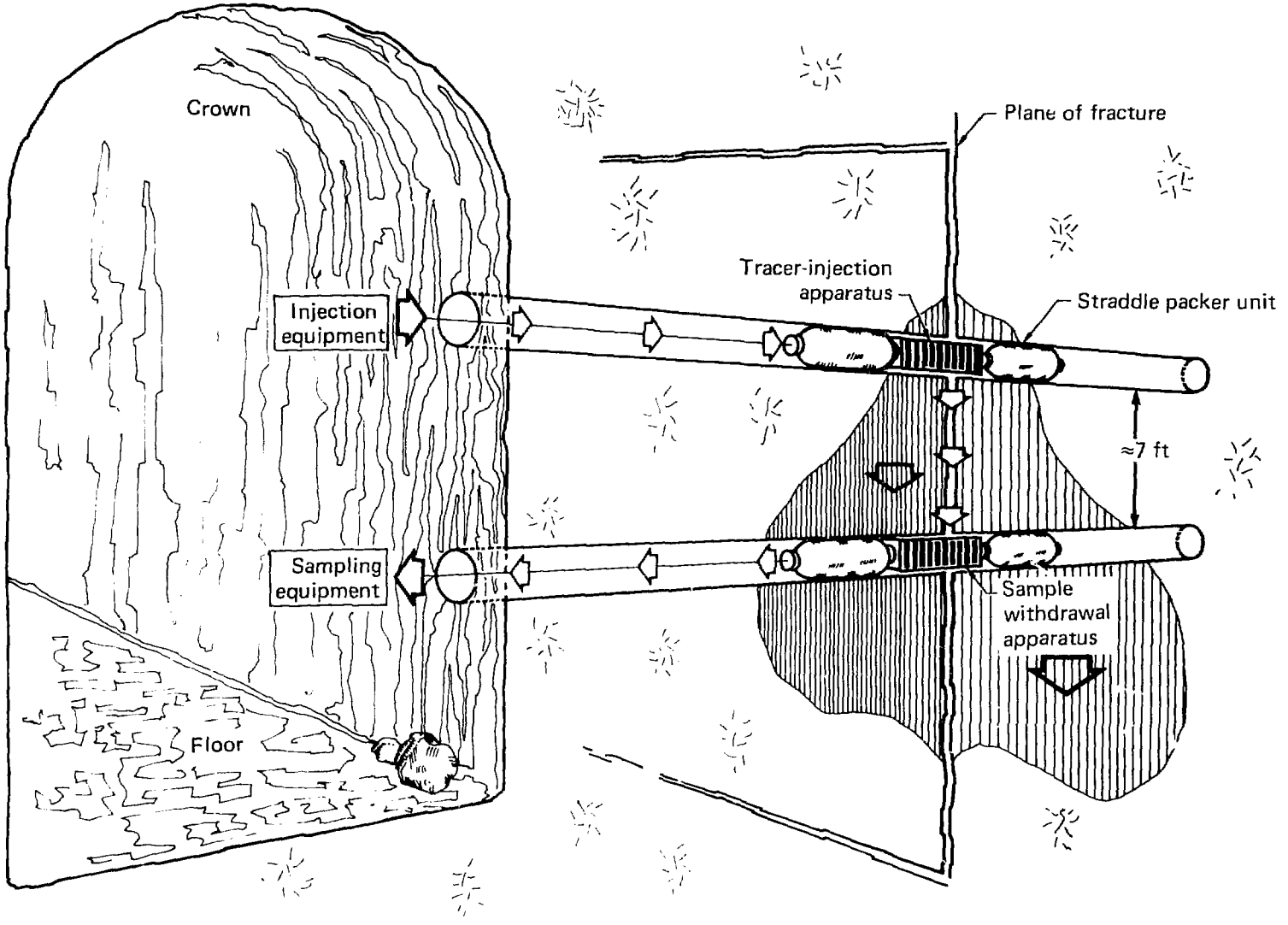

Figure 1. Conceptual design for field migration studies.

2. A solution of ground water containing tritium and ^{36}Cl (see Sec. 3.4) will be injected into the flow. Samples will be automatically collected at preset intervals and analyzed on-line by flow through the β^- detector. When the tritium and ^{36}Cl peaks have passed, we will know both the time of travel between the inlet and outlet holes and be able to calculate dilution and dispersion. This will allow us to make an informed estimate of the amounts of sorbing radionuclides to be injected so that the collected samples are within the sensitivity range of the detectors and give good time resolution (see Sec. 3.4).
3. A solution of ground water containing a nonsorbing radionuclide (^{3}H or ^{36}Cl) and ^{85}Sr, ^{137}Cs, and ^{99}Tc (or ^{95m}Tc, depending on availability) will be injected into the flow. The outlet flow will be analyzed on-line by both β^- and γ detectors. Samples will be automatically collected when any of the radionuclides is detected in the outlet flow. The time each peak is eluted relative to the nonsorbing nuclide will give a direct measure of the retardation factor. It is possible that the single pulse injection will produce a poorly defined peak because of dilution by mixing, dispersion, poor recovery at the outlet hole, loss into connecting fractures, or nonequilibrium sorption kinetics. An alternative is continuous injection where a spiked solution of constant concentration is injected for a period of time equal to or greater than the travel time of a nonreactive tracer. The ratio of the concentration at the outlet to the original concentration (C/C_0) plotted against time should produce an S-shaped curve starting at $C/C_0 = 0$ and ending at C/C_0 approaching unity (see Sec. 4.2). The time at $C/C_0 = 0.5$ is equivalent to the peak time in the single pulse injection method and can be used to calculate a retardation factor in a similiar way.

   The field experiment will continue until we have adequately defined the shape of the elution curve for each radionuclide as determined by the on-line detectors or until the time elapsed greatly exceeds that predicted for migration to occur. This time will be based on both the laboratory experiments and the results of the earlier field experiments described in step 2.

4. At the end of the first experiment there will be a second injection of radionuclides into the same fracture, provided we have been able to recover the nonsorptive tracer and at least one of the sorbed radionuclides. Only those radionuclides that have been eluted will be reinjected. This will give us duplicate retardation factors for some radionuclides while allowing the experiment to continue to run with the hopes of eventually eluting the radionuclides that have higher retardation. Other fractures will also be studied if the first set of experiments has gone smoothly and in a relatively short period of time. This will allow us to study the variability between fractures. Our apparatus is designed so that approximately 1 week is required to move from one experimental site in the drift to another. We estimate that 6 months are needed for the injection--collection phase of this study.
5. At the end of the injection phase we will back-core into the fracture between the inlet and outlet hole. Samples containing the fracture will be studied to detect the presence of radionuclides that have either precipitated or are still in the process of migrating through the fracture. The position of radionuclides remaining in the fracture will allow us to calculate a retardation factor, providing that a peak concentration can be found and the material is not simply distributed somewhere along the fracture. This might occur if precipitation rather than sorption takes place as could be the case with technetium.

There are two major problems that need to be solved in the laboratory prior to the back-coring activity. First, we need to find a cementing agent that can be injected into the fracture to prevent radionuclides that have sorbed or precipitated onto the fracture filling material from being washed out with drilling water. If we fail to identify a suitable cementing agent, an alternative method will be to mine back close to the fracture and then core the rock without fluids using drills similar to those used in sampling rock for paleomagnetic studies. Second, to determine the flow field, we need to select a dye to be injected into the fracture that will stain the fracture filling material, but will not interact with the radionuclides in the fracture. By drilling a series of holes across and down the fracture we

can bound the extent of the flow field by the presence or absence of the dye. Dying the surface of the flow field is considered necessary since (1) it's unlikely the sorbed radionuclides will be evenly distributed along the flow field and (2) the activity of the radionuclides remaining behind on the surface may be below the dectection limits of the analytical techniques.

At the end of the migration experiments and the supporting subtasks a final report will be written that compares the field and laboratory work, discusses the capabilities of the pretest predictions, and makes recommendations for the use of similar tests on other rock types.

3.2. EXPERIMENTAL FACILITY

The Climax Stock is a composite granitic intrusive body located at the northern end of the Nevada Test Site (Fig. 2). The composite stock is of Cretaceous age and intrudes paleozoic sediments and metasediments. The majority of the exposed wall rocks are Ordovician limestones and dolomites of the Pogonip Group. The stock also intrudes the Eleana Formation, a series of argillites, limestones, and quartzites of Carboniferous age and the Cambrian Stirling Quartzite [Houser and Poole (1960)]. The stock and the rocks it intrudes are overlain by the Tertiary pyroclastic rocks of the Oak Spring Formation. The stock itself is intruded by numerous aplite and pegmatite dikes. The underground workings at the Spent Fuel Test level, shaft 1501, provide access to this granitic mass at a depth (420 m) comparable to that being considered for geologic disposal of nuclear waste materials. Figure 3 is a map of the Spent Fuel Test level and location of the drift where the radionuclide migration experiments will take place.

The Climax granitic stock is composed of two main units (granodiorite and quartz monzonite) and contains numerous fractures and local faults. The level at which this experiment will be conducted is apparently above the saturated zone [Murray (1981)]. Based on analysis of known geological and hydrological data, Murray concludes the water table probably lies at 975 m mean sea level (MSL) beneath the location of the Spent Fuel Test (i.e., approximately 145 m below the experimental area). Ground-water seeps from isolated fractures into the drift are attributed to overflow from perched water locations.

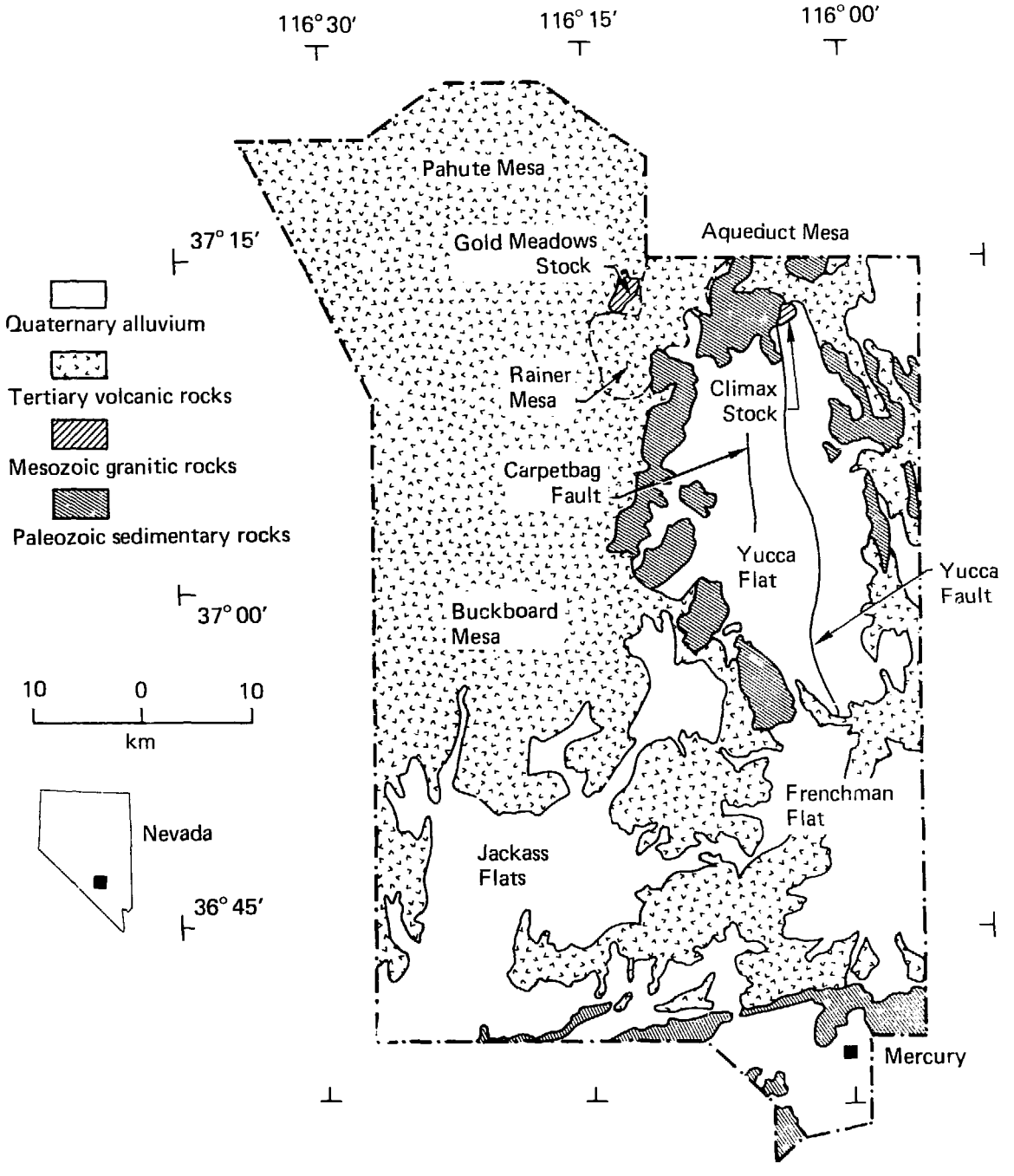

Figure 2. Principal rock types and test areas at the Nevada Test Site.

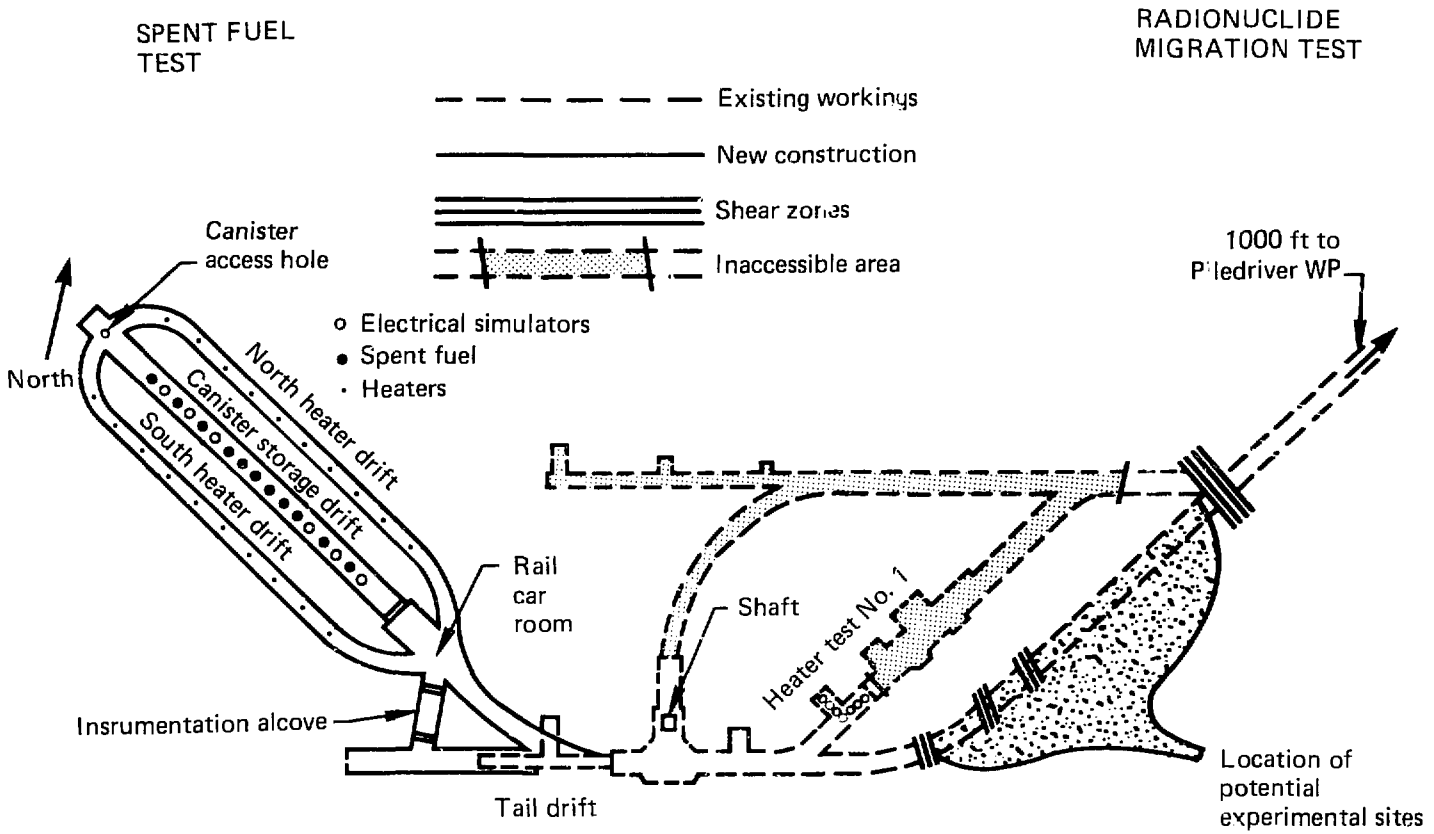

Figure 3. This map of underground workings at Spent Fuel Test Level Shaft 1501 in Climax Mine, NTS, shows location of potential experimental sites for field migration studies.

3.3. FRACTURE MAPPING

Detailed fracture mapping in the Piledriver Drift was done by Thorpe and Springer (1981). The predominant orientation of the fractures is N50W/90 (strike/dip). A somewhat lesser peak within this clustering is oriented N25W/85SW. These correspond roughly to the NW-striking fault and joint sets reported by Maldonado (1977), as well as to some of the shear zones and joints given by Wilder and Patrick (1980). Typical mineralization of fractures in the main access drift is mostly calcite, with some iron oxide and chlorite. The wall rock is sometimes altered to clay. Thickness of filling varies widely both on a given fracture and among fractures, but for single unsheared features it is typically 1 to 3 mm.

Another prominent grouping of high-angle fractures is oriented N45E/87SE and corresponds to the NE-striking set of high-angle fractures reported by Maldonado (1977) and Wilder and Patrick (1980). These fractures also appear to be filled with mostly calcite and minor amounts of clay and iron oxide. A third set of discontinuities was observed in the access drift with a mean orientation of N35W/25NE. This subhorizontal set is apparently pervasive in the Climax Stock. Most of these features are planar and healed by quartz up to 10 mm thick. They typically contain pyrite in either continuous veinlets or discontinuous stringers. They tend to break or be open where the pyrite is continuous.

3.4. RADIONUCLIDE SELECTION

To simplify the solution chemistry in the tracer, we will use only the following radionuclides in the first set of experiments: ^{3}H, ^{36}Cl, ^{99}Tc, ^{95m}Tc, ^{85}Sr, and ^{137}Cs. Table 1 gives estimates of the amount of each radionuclide needed to provide a good signal from the β^- or γ on-line detectors at the outlet hole.

To calculate the estimates for total mCi to be injected, the detection limits were multiplied by a factor of 10^4 for ^{3}H and ^{36}Cl, 10^5 for ^{99}Tc, ^{95m}Tc, and ^{85}Sr, and 2.5×10^5 for ^{137}Cs to account for:

- The initial dilution when 10 ml of tracer solution are injected into the straddled interval (vol = 100 ml), i.e, ~10 to 1.

Table 1. Estimated amounts of radionuclides.

Nuclide	Detection limit (dpm/ml)	Input concentration (dpm/ml)	Total mCi in 10 ml of tracer solution
^{3}H	1000	10^{7}	0.05
^{36}Cl	100	10^{6}	0.005
^{99}Tc	100	10^{7}	0.05
^{95m}Tc	100	10^{7}	0.05
^{85}Sr	500	5×10^{7}	0.25
^{137}Cs	200	5×10^{7}	0.25

- The broadening of the peak because of sorption--desorption kinetics within the fracture, which assumes a factor of 10 to 1.
- The loss from sorption onto the walls of equipment, dispersion within the injection lines, etc., which assumes a factor of 10 to 1 for all radionuclides except for ^{137}Cs, which is 25 to 1, and ^{36}Cl and ^{3}H, which are not affected.
- A factor of 100 above the detection limit of the on-line detectors to produce good counting statistics.

It should be emphasized that the estimates, with the exception of ^{3}H and ^{36}Cl, are for planning purposes only. A final determination of the amounts of each nuclide needed will be calculated after the first migration test using the nonsorptive tracers. Tritium was selected to provide a measure of the dilution and transit time for the tracer through the inlet apparatus, the fracture, and the outlet apparatus. With this information, retardation of sorptive tracers can be quantitatively determined by comparison of arrival times. Initial flow tests with ^{3}H will provide the necessary dilution information for selecting the activity levels required for the other radionuclides.

Chlorine-36 was chosen to provide a second nonreactive tracer as a comparison to ^{3}H. The advantages of ^{36}Cl are its long half-life (3×10^{5} y) and its stability in water. The disadavantage of ^{36}Cl is that it has no analog in nuclear waste.

Strontium-85 was chosen to represent the behavior of the important waste component ^{90}Sr. The use of ^{85}Sr allows for direct gamma counting. This avoids the need for expensive radiochemical techniques required for the analysis of ^{90}Sr. Strontium-85 has been used extensively for both our laboratory batch and core sorption studies.

Technetium-99 was chosen because it is a very important long-lived component of nuclear waste. Its geochemical behavior is interesting because it can either be mobile as the TcO_4^- anion or precipitate as TcO_2, given reducing conditions in the ground water [Bondietti and Francis (1979)]. In the laboratory under atmospheric conditions, ^{95m}Tc has been observed to migrate with ^{3}H through Climax granite rock cores. Only a small component (0.1 to 0.5%) stayed with the core. It was probably reduced to TcO_2 by ferrous iron in the rock. Although ^{95m}Tc can be gamma counted directly, it may not be used in the field experiments since the cost and availability depend on the amount being produced by the supplier (New England Nuclear, Boston, MA) at the time it is ordered. The alternative, ^{99}Tc, although readily available, must be analyzed by liquid scintillation and can interfere with the tritium analysis.

Cesium-137 is an important short-lived component of waste. It has shown moderate sorption in laboratory experiments and its behavior in the field is of interest for comparison to the laboratory data. Cesium-137 is easily analyzed by direct gamma counting and it is an available and inexpensive isotope. Table 2 summarizes the characteristics and analytical methods to be used with the various selected radionuclides.

To keep the nuclear chemistry as simple as possible, we have not included the actinides in these initial migration experiments. Plutonium in particular was not selected since laboratory studies have shown it to be so easily sorbed by most rocks and minerals that it is essentially immobile. As it is not expected to move, the extra experimental problems it generates make its use impractical for an initial test. Until we can prove that the migration experiments are feasible, safe, and give valid results, the use of actinides is not warranted. The increased costs related to actinide production and radiation safety requirements would pull funds away from our primary mission of developing techniques for studying radionuclide migration in the field. At the successful completion of this project, we will propose a second series of experiments designed to handle actinides.

Table 2. Selected radionuclides.

Radionuclide	Half-life	Decay mode	Analysis method
^{3}H	12.3 y	β^-	Liq. scin.[a] 18.6 keV β^-
^{85}Sr	64.8 d	EC[b]	γ-count 514 keV γ
^{95m}Tc	61.2 d	EC	γ-count 204 keV γ
^{99}Tc	2.14×10^{5} y	β^-	Liq. scin. 292 keV β^-
^{137}Cs	30.17 y	EC	γ-count 661.6 keV γ
^{36}Cl	3.0×10^{5} y	β^-	Liq. scin. 709 keV β^-

[a]Liq. scin. = liquid scintillation technique.
[b]EC = electron capture.

3.5. LABORATORY SUPPORT STUDIES

Retardation factors calculated from the results of the field experiments will be compared to values measured in laboratory core sorption experiments. The laboratory study uses Climax granite rock cores containing both natural and artificial fractures for a comparison of the retardation effects of the fracture fill material. The cores are held under confining pressure in the core sorption apparatus described in Weed et al. (1981). Natural Climax ground water is pumped through the core and a tracer solution containing the same radionuclides we plan to use in the field is injected into the core. Samples are collected and analyzed. Laboratory activities to date have concentrated on upgrading equipment, modifying the sorption apparatus for fractured cores, and testing the equipment in a series of sorption experiments [Failor et al. (1982)].

The core sorption study is a logical step in determining the scaling factors of laboratory to field studies. We need to determine whether laboratory studies accurately reflect in situ conditions. Results from the laboratory experiments will also be used in the hydrologic models to make pretest predictions in addition to those described in Sec. 4.2.

In addition to the core sorption experiments, there will be a detailed study of the fracture fill material. Although the physical properties (e.g.,

density, thermal conductivity, compressive strength) of the Climax granite are similiar to those of other granitic rocks [Ramspott et al. (1979)], the petrography of the fracture fill material is atypical. Instead of the secondary clay minerals usually found in fractures at depth in granite, the Climax high-angle fractures have a relatively thick (1 to 3 mm) calcite deposit similar to that found in rock fractures near the surface.

We need to study the sorption characteristics of calcite in both the core sorption experiments described above and in batch sorption experiments using only the fracture fill material as the sorbent. We also need to study the alteration of the rock immediately adjacent to the fractures. If alteration has occurred, this could affect the local porosity and thus the extent of matrix diffusion. Other laboratory work will be designed as needed to answer specific questions that will help us understand the results of the field experiments.

4. HYDROLOGICAL INVESTIGATIONS

4.1. FRACTURES OF POTENTIAL USE IN TRACER EXPERIMENTS

Initial field activities concentrated on hydrological investigations to evaluate the flow characteristics of the fractures and determine whether fractures in the Climax Stock are suitable for radionuclide migration experiments. To date, borehole pairs have been drilled at three sites in the drift. Each borehole was visually logged using a high-quality optical borescope with a 35-mm camera attachment for photodocumentation. Fractures were selected for testing that were at least one tunnel diameter away from the drift wall to avoid the fractures induced by mining. The inflatable straddle packer assemblies, used to isolate individual fractures, were modified to measure pressure in the packed-off interval. Because the fracture characteristics were unknown, hydraulic test equipment was designed to provide and monitor a wide range of injection pressures and flow rates [Raber et al. (1982)].

This equipment was used to conduct both hyraulic and recovery tests on the fractures. The hyraulic tests were designed to provide input data for hydrologic models to determine fracture apertures and intrinsic permeabilities. The recovery tests were used to determine the interconnecting fractures between the upper and lower boreholes. They were done by setting the packer in the upper borehole to isolate a particular fracture. Water was pumped into the fracture and the borescope was used to visually determine whether water was dripping from any one fracture in the lower borehole. Once this interconnection was proved, the second packer was placed in the lower borehole to isolate that fracture. The recovery rate was determined by comparing the amount injected to that measured for the return flow as a function of the input pressure.

In two pairs of boreholes (TT1-TT2 and TT5-TT6), a total of 14 fractures have been tested at this time. A summary of the results and the location of the fractures within the boreholes are shown in Figs. 4 and 5. Fractures were not tested in the third pair of boreholes (TT3-TT4) because high-angle fractures identified in the upper borehole could not be correlated to fractures seen in the lower borehole. Out of the 14 fractures tested, two potentially useful near-vertical fractures at 547 cm in TT2 and

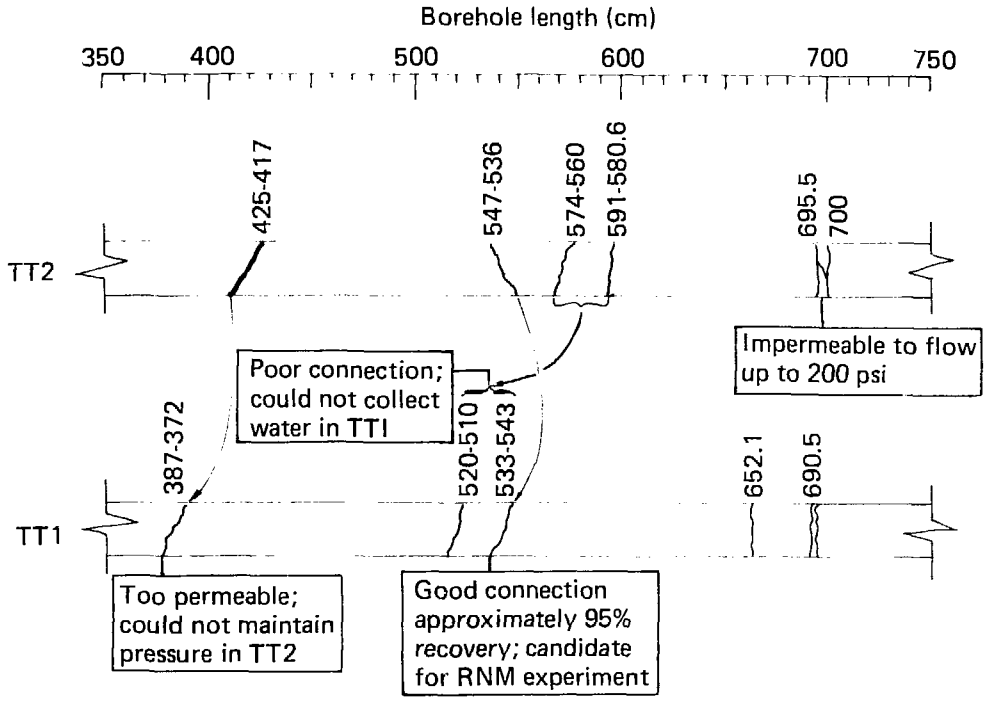

Figure 4. Summary of hydraulic tests in boreholes TT1 and TT2.

870 cm in TT6 were identified as providing good connection between the boreholes. Injection of water into the fractures in the upper boreholes using straddle packers has resulted in flow through the fractures to the lower boreholes with up to 95% of the injected water volume being recovered.

Prior to the hydraulic tests, filtered water was injected into the fractures to assure that they were water saturated in the vicinity of the boreholes. (The fractures normally are unsaturated with respect to water.) The primary test procedure consisted of injecting water into the fractures through the upper boreholes at constant injection pressure over a period of 5 to 6 h. The lower holes were closed off so that no flow occurred out of the fractures. The injection flow rates declined with time in a systematic manner. This flow rate decline was used to estimate the effective fracture aperture widths using a radial nonsteady flow model as described by Jacobs and Lohman (1952). The flow rate decline in one of the tests is shown in Fig. 6, where S_w is the constant injection head, r_w is the radius of the borehole, Q is the injection flow rate, and t is time.

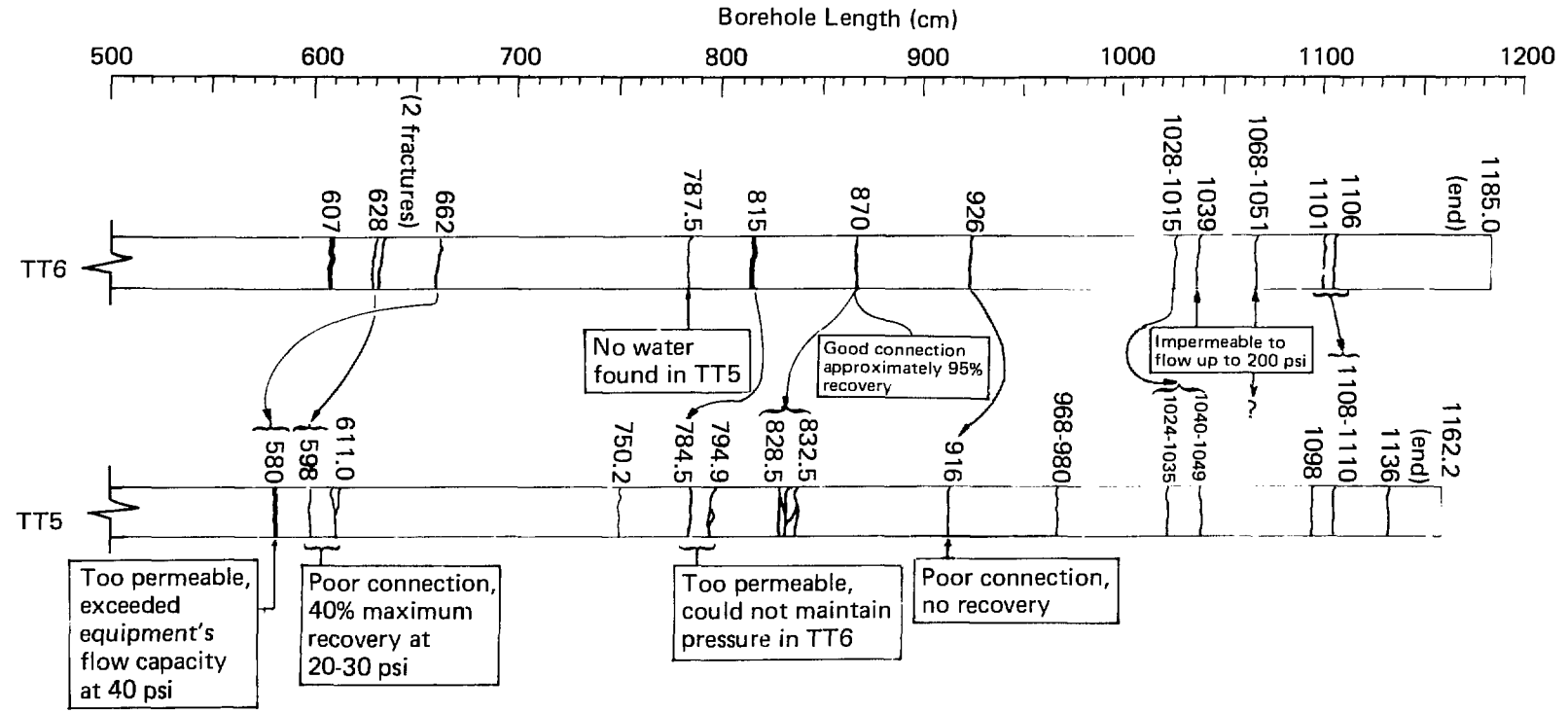

Figure 5. Summary of hydraulic tests in boreholes TT5 and TT6.

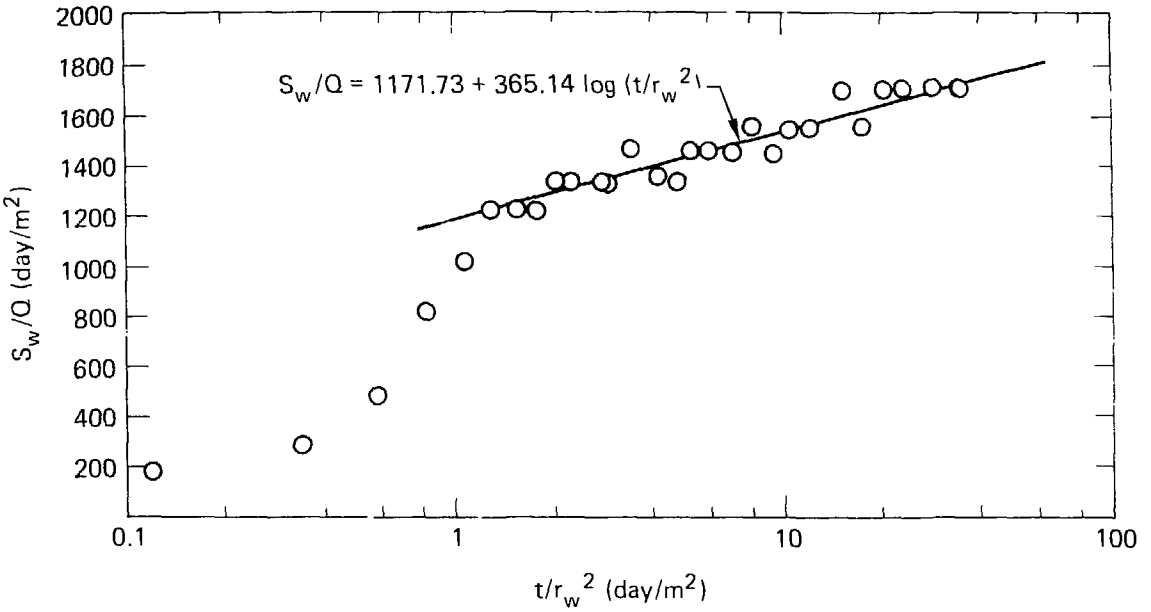

Figure 6. Flow-rate decline during injection into TT6 at constant 67 psig pressure, January 7, 1981.

The transmissivity of the fractures was calculated from:

$$T = \frac{2.3}{4\pi\Delta(S_w/Q)} \quad , \tag{1}$$

as given by Jacob and Lohman, where $\Delta(S_w/Q)$ is the change in S_w/Q per log cycle of t/r_w^2 according to the equation of the best-fit line through the test data. The effective fracture widths b were calculated using a rearrangement of:

$$T = Kb = \frac{k\rho gb}{\mu} = \frac{b^2\rho gb}{12\mu} \quad , \tag{2}$$

where K is hydraulic conductivity, k is intrinsic permeability, ρ is water density, and μ is water viscosity.

Analysis of test results provided effective fracture aperture width estimates of 20 and 30 μm, respectively, for the fractures tested in boreholes TT6 and TT2. These values correspond to intrinsic permeabilities of 33 and 75 $(\mu m)^2$. The Jacob and Lohman radial flow model is based on horizontal flow, but is thought to be a reasonable vehicle to use in our test analyses where the applied injection pressure gradients, based on injection pressures

of 47 and 67 psig, are large relative to the hydrostatic pressure gradient. The systematic flow rate decline during the tests is that expected in a saturated system and suggests that we were successful in saturating the fracture locally.

Borehole to borehole injection tests were also done on the two fractures to test whether the interborehole hydraulic properties were different because of channeling or fracture aperture anisotropy from those inferred using the single borehole tests. The borehole to borehole tests used the same procedure as that described for the recovery tests.

The equation that describes the steady radial flow of water from an injection well in a horizontal fracture according to the simple parallel plate model was used to estimate the effective fracture aperture. Equation (3):

$$Q = \frac{2\pi(b)^3 \rho g \ (h_w - h_e)}{12\mu \ \ln\left(\frac{r_e}{r_w}\right)} \quad , \tag{3}$$

where h_w is the head at the injection hole, h_e is the head at the outlet hole, r_w is the radius of the injection hole, and r_e is the radial distance to the outlet, can be rearranged to yield:

$$b = \left[\frac{6Q\mu \ \ln\left(\frac{r_e}{r_w}\right)}{\pi \rho g \ (h_w - h_e)}\right]^{1/3} \quad . \tag{4}$$

The test involved essentially vertical flow from the injection hole, but the applied pressure head was large relative to the static pressure difference between the injection and outlet holes. We realize our flow pattern from the injection hole was not symmetrically radial, but the model is still adequate for estimates of b.

The fracture apertures were estimated using several flow rates. The calculated values of 20 and 27 μm for the apertures of the two fractures in TT6 and TT2 are in good agreement with the estimates from the nonsteady injection tests described previously (i.e., 20 and 30 μm).

Independent analysis of the hydraulic tests of the fractures by Intera Environmental Consultants, Inc., Houston, TX [R. Lantz, personal communication

(1981)] is still progressing but the results confirm our estimates of average fracture aperture width. Intera has found that it is necessary to treat the fractures as only partially water saturated with a connecting matrix to reproduce the test results with their analytic and numerical models. They estimate the fracture saturation radius to be at least 6 m around the injection point in the fractures.

4.2. PRETEST PREDICTIONS OF SOLUTE TRANSPORT AND DILUTION

Using several simple analytical solutions to the problem of solute transport in single fractures, estimates of tracer dilution and travel time in the planned experiments have been derived. Three fracture widths were considered: 10, 20, and 30 μm. The 20-μm fracture is the most likely to be used. We have yet to find a fracture less than 20 μm in aperture width that gives good return flow.

The first estimates of tracer dilution and travel time come from the analysis of the flow field in the vicinity of a recharging-discharging well pair [Morrison (1982)]. The solution deals with the dispersion that results from the tracer arrivals occurring at different times along different curved flow paths between the injection and outlet holes, assumed to be 1.5 m apart. It predicts the conditions for breakthrough of radionuclides at the outlet hole and describes the concentration history of fluid flowing from the fracture. Injection into the vertical fracture through one borehole, coupled with extraction from the second hole at the same volume flow rate Q in a fracture that is water saturated only between and in the vicinity of the boreholes, is assumed to be a system equivalent to that in a fully water-saturated fracture with a superimposed uniform downward flow.

The stream function describing the streamlines for the latter case is:

$$\psi = \frac{Q}{2\pi b} \tan^{-1} \frac{-2ay}{x^2 + y^2 - a^2} + Vy \quad , \tag{5}$$

where a is half the distance between boreholes, V is the uniform downward flow velocity, and x and y are orthogonal coordinates. The streamlines connecting the boreholes are in this case entirely contained within a boundary, an oval-shaped streamline. Fluid injected into the fracture will flow to the extraction borehole on any of these streamlines. The time to

traverse between boreholes will depend strongly on the particular streamline path followed by the fluid. The longer streamlines are also those with low fluid velocity.

Corresponding to the stream function is the complex potential:

$$\Omega = \frac{Q}{2\pi b} \ln \frac{z + a}{z - a} + Vz \quad . \tag{6}$$

The streamline function is the imaginary part of this complex potential. The complex velocity is:

$$w = \frac{d\Omega}{dz} = V - \frac{Qa}{\pi b\,(z^2 - a^2)} \quad . \tag{7}$$

The fastest trip between boreholes is along the straight line connecting them. Using Eq. (7) to evaluate the time:

$$t = \int_{-a}^{a} \frac{dx}{V} \quad . \tag{8}$$

The real component of w is the x component of velocity. Along this streamline there is no y component.

$$t = \int_{-a}^{a} \frac{dx}{V - \dfrac{Qa}{\pi b\,(x^2 - a^2)}} \quad . \tag{9}$$

Integrating gives:

$$t = \frac{2a}{V} \left[1 - \frac{\dfrac{Q}{\pi ba\,V}}{\left(1 + \dfrac{Q}{\pi ba\,V}\right)^{1/2}} \coth^{-1} \left(1 + \frac{Q}{\pi ba\,V}\right)^{1/2} \right]$$

or

$$\text{volume} = \frac{2Qa}{V} \left[1 - \frac{\dfrac{Q}{\pi ba\,V}}{\left(1 + \dfrac{Q}{\pi ba\,V}\right)^{1/2}} \coth^{-1} \left(1 + \frac{Q}{\pi ba\,V}\right)^{1/2} \right] \quad . \tag{10}$$

Letting $Q/\pi ba\,V$ increase without bound in Eq. (10) yields:

$$t = \frac{4\pi ba^2}{3Q}$$

and $$\text{volume} = \frac{4\pi ba^2}{3} \quad , \tag{11}$$

which gives the breakthrough time for a tracer along the path connecting boreholes and the volume injected at breakthrough, respectively.

Following breakthrough (initial appearance of tracer at the withdrawal hole), the concentration of tracer arriving at the withdrawal hole will increase. The arriving concentration ratio is given by:

$$f = \frac{2\text{Im}\,(\Omega)b}{Q} + 1 \quad . \tag{12}$$

Integrating velocity along this streamline yields the time at which this concentration is obtained. In dimensionless form, such integration produces:

$$C/C_0 = C/C_0 \left(\frac{Q}{\pi ba\ V}, \frac{tV}{a}\right) \tag{13}$$

or because volume is Q X t:

$$C/C_0 = C/C_0 \left(\frac{Q}{\pi ba\ V}, \frac{\text{volume}}{4\pi ba^2}\right) \quad . \tag{14}$$

Numerical integration in the complex plane was used to obtain results in this form. A family of curves is produced, corresponding to different values of dimensionless flow rate. The curves represent C/C_0 as a function of the volume of fluid injected into the injection borehole. From the appropriate curves the breakthrough concentration history of a tracer in the injected flow can be constructed.

All of the following estimates of tracer transport assume an injection pressure of only 3 psig and injection of 100 ml of tracer solution. The estimates of nonreactive tracer pulse arrival at the outlet hole are shown in Figs. 7 to 9. The estimates by the method of Morrision show that even in the case of the 30-μm fracture, there is little tracer dilution in the fracture. (There is a 10X dilution of the initial 10 ml of tracer solution as it is initially mixed with about 100 ml of water in the packed-off interval in the inlet hole.) In the 10-μm fracture the tracer pulse arrives

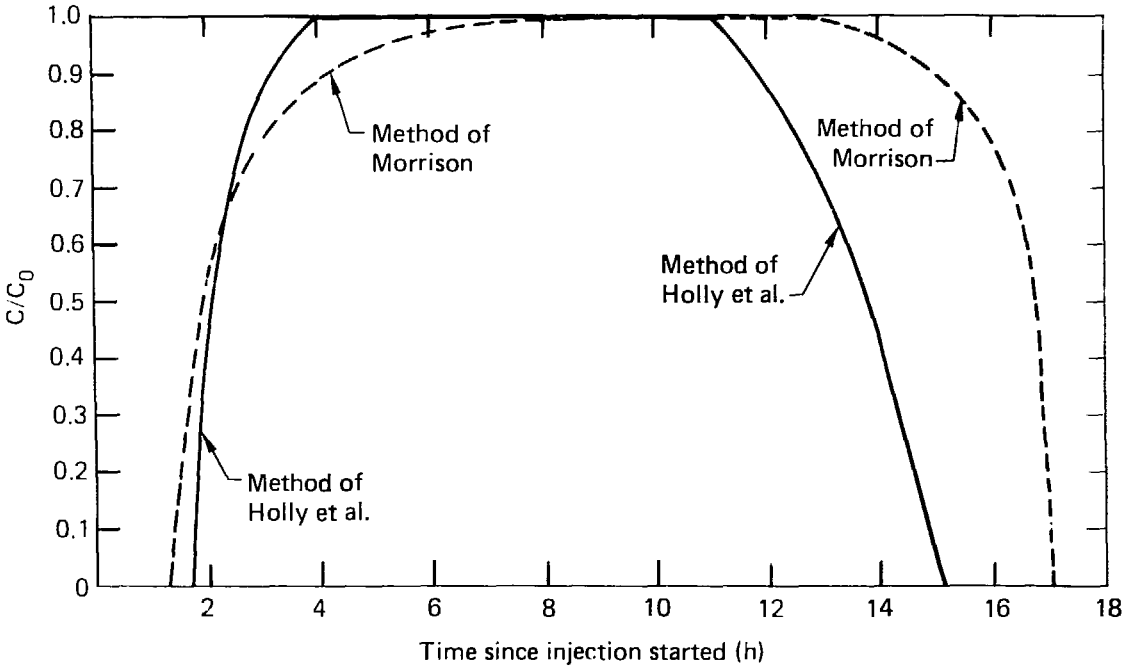

Figure 7. Nonreactive tracer pulse arrival at outlet hole with flow through 10-μm fracture.

at the outlet hole as a rather long pulse that remains at near the input concentration for several hours.

A second series of tracer pulse arrivals at the outlet hole was estimated using a solution to the one-dimensional transport equation developed by Holly et al. (1971). The equation, describing one-dimensional solute transport in saturated ground-water systems, is:

$$B \frac{\partial c}{\partial t} + B\lambda C - D \frac{\partial^2 C}{\partial x^2} + V \frac{\partial c}{\partial x} = 0 \quad , \tag{15}$$

where: $B = 1 + \left(\frac{1 - \phi}{\phi}\right) K_{dv}$, a retardation factor,

K_{dv} = volume distribution coefficient,
λ = radioactive decay constant,
C = concentration of solute,
D = coefficient of dispersion,
V = water flow speed,
X = distance in flow direction, and
ϕ = porosity of medium.

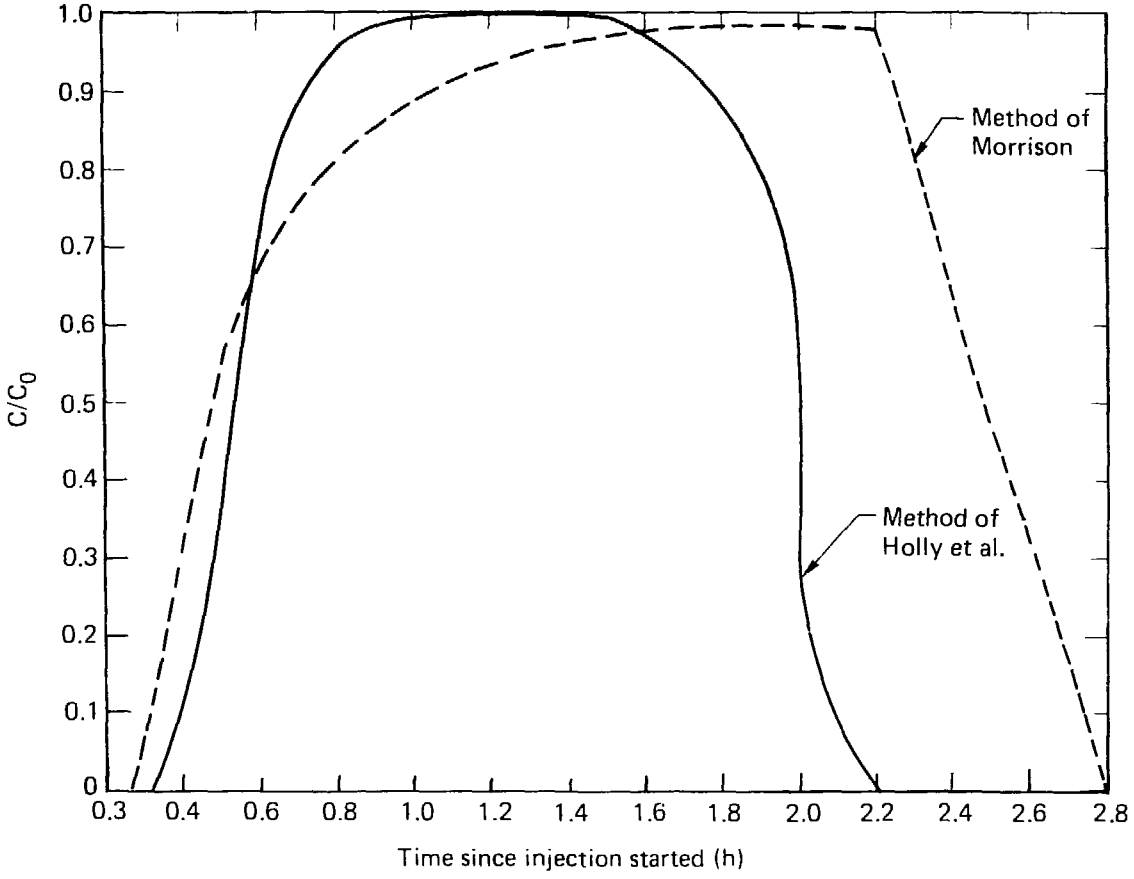

Figure 8. Nonreactive tracer pulse arrival at outlet hole with flow through 20-μm fracture.

This equation takes into account the effects of radioactive decay, sorption, advection, and dispersion on the distribution of tracer concentration in time and with distance away from the point of introduction.

With the initial condition that:

$$C(x,0) = 0 \text{ for } x > 0$$

and the boundary conditions that:

$$C(x,t) \longrightarrow 0 \text{ as } x \longrightarrow \infty, \; t \geq 0$$

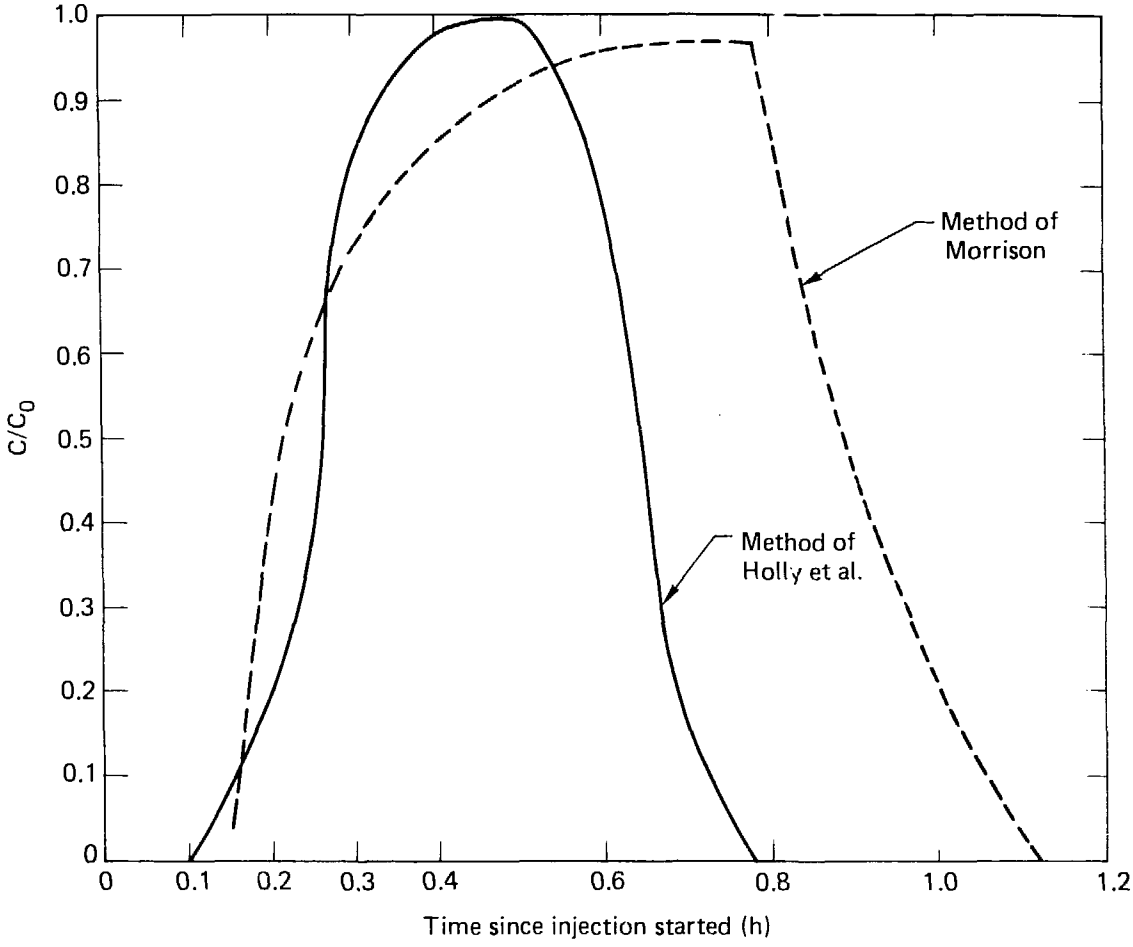

Figure 9. Nonreactive tracer pulse arrival at outlet hole with flow through 30-μm fracture.

and $$C(0,t) = C_{0,0} \exp(-\lambda t),\ 0 \leq t \leq t_0$$

$$C(0,t) = 0,\ t > t_0 \quad ,$$

where t_0 = time required to inject tracer pulse:

$$C_{0,0} = C(x,t) \text{ at } x = 0,\ t = 0 \quad ,$$

the solution of the transport equation is [Holly et al. (1971)]:

$$C(x,t) = 1/2\ C_{0,0}\ \exp\ (-\lambda t)\ \left\{\text{erfc}\left[\frac{x - Vt/B}{2(Dt/B)^{1/2}}\right] + \exp\left(\frac{Vx}{D}\right)\right.$$

$$\left. \cdot\ \text{erfc}\left[\frac{x + Vt/B}{2(Dt/B)^{1/2}}\right]\right\}$$

for $t \leq t_0$ and

$$C(x,t) = 1/2\ C_{0,0}\ \exp(-\lambda t)\ \left[\text{erfc}\left[\frac{x - Vt/B}{2(Dt/B)^{1/2}}\right] - \text{erfc}\left\{\frac{x - V(t - t_0)/B}{2\left[D(t - t_0)/B\right]^{1/2}}\right\}\right.$$

$$\left. + \exp\left(\frac{Vx}{D}\right)\left(\text{erfc}\left[\frac{x + Vt/B}{2(Dt/B)^{1/2}}\right] - \text{erfc}\left\{\frac{x + V(t - t_0)/B}{2\left[D(t - t_0)/B\right]^{1/2}}\right\}\right)\right] .$$

for $t > t_0$ (16)

The pulse arrivals for a nonreactive tracer estimated by the method of Holly et al. for a 10-, 20-, and 30-μm fracture are also illustrated in Figs. 7 to 9. Dispersion was accounted for by assigning a value of 0.04 m to longitudinal dispersivity in the fracture. Grisak et al. (1980) found that a dispersivity value of 0.04 m provided enough dispersion to adequately simulate a solute transport experiment in a 40-μm fracture. The arrival of the peak of the pulse is predicted to be somewhat sooner in each fracture by the method of Holly et al., but as with the method of Morrison, very little dilution of the tracer occurs in its short travel in the fracture. It is thought that the tracer pulses of reactive solutes will show a somewhat more gradual decline in concentration than shown by the nonreactive tracer. Sorption-desorption kinetics of the reactive tracers may contribute to this.

Table 3 summarizes the pulse transport prediction for the three fracture widths considered. The pulses result from injection of 100 ml of tracer solution under the same conditions used to generate the pulses shown in Figs. 7 to 9. The average water flow speed is that calculated from:

Table 3. Tracer pulse transport in single fracture.

Average fracture aperture (μm)	Average water flow speed[a] (m/h)	Time to inject 100-ml tracer solution (h)	Time for pulse peak to travel 1.5 m (h)		
			No sorption[b]	Sr	Cs
10	0.70	11.1	2	430	6000
20	2.8	1.4	0.6	54	750
30	6.4	0.4	0.25	16	219

[a] Based on 3-psig injection pressure.

[b] Based on pulse arrival prediction after Holly et al. (1971).

$$V = b^2 \frac{\rho g}{12} \frac{dh}{dl} \quad , \tag{17}$$

where dh/dl is the hydraulic gradient in the fracture. The time required to inject 100 ml of tracer solution was estimated assuming a 3-psig injection pressure and a fracture aperture width using:

$$Q = \frac{\pi (b)^3 \rho g \, (h_w - h_e)}{12 \mu \ln \left(\frac{r_e}{r_w} \right)} \quad , \tag{18}$$

from the method of Morrison where:

h_w = hydraulic head at injection point,
h_e = hydraulic head at outlet hole,
r_w = radius of injection hole, and
r_e = distance from injection point to outlet hole.

The time for the pulse peak to travel 1.5 m in the fracture was estimated by subtracting one half the time to inject 100 ml of tracer solution from the time of arrival of the tracer pulse as shown in Figs. 7 to 9 after Holly et al. These times are very close to those obtained by dividing 1.5 m by the average water flow speed for unretarded ion transport.

The retardation factor (the ratio of the water velocity to that of a solute) for flow in a fracture, where matrix diffusion is ignored and the only sorption is that on the fracture surfaces, is given by [Tang et al. (1981)]:

$$R = \frac{1 + 2K_a}{b} \quad , \tag{19}$$

$$K_a = \frac{\text{mass solute on surface/surface area}}{\text{mass solute in solution/volume of solution}}$$

where R equals a retardation factor calculated using a surface distribution coefficient (K_a). This equation assumes reversible sorption, chemical equilibrium, and a linear sorption isotherm.

According to Neretnieks (1980):

$$K_a = \frac{K_d \rho_p}{a} \quad , \tag{20}$$

where: K_d = the bulk distribution coefficient,
ρ_p = bulk density of rock, and
a = specific surface (area of fractures or particles divided by volume of rock).

Therefore K_a is proportional to K_d. We have measured K_a in the laboratory for ^{90}Sr on thin sections from Climax granite with an average value of 0.001 m^3/m^2. Our measurements of K_d in the laboratory for strontium and cesium on Climax granite yield a value of 21 for ^{85}Sr and 306 for ^{137}Cs. Using the 21 to 306 ratio of Sr to Cs sorption, we assume a K_a for cesium of 0.014 m^3/m^2. The travel times for strontium and cesium peaks as given in Table 3 were estimated from these K_a values and the fracture flow retardation coefficients.

The reactive solute tracer pulse travel times given in Table 3 are at the estimated times required with various solutes and fractures to see pulse arrivals. The uncertainty in these times is unknown. We have very few

laboratory measurements of K_a to work with and those that are available were made on fresh granitic surfaces, not on weathered and altered fracture surfaces and fracture filling material. Furthermore, it is not known how reasonable it is to scale K_a values for solutes from their K_d values.

Tracer breakthrough, assuming a source of constant concentration for the 20-μm fracture, was estimated using the model of Tang et al. (1981). The model accounts for sorption on the fracture surfaces as well as diffusion of solute into the matrix of the rock and sorption there. The transport processes in a fracture are described by:

$$\left.\frac{\partial C}{\partial t} + \frac{V}{R}\frac{\partial C}{\partial z} - \frac{D}{R}\frac{\partial^2 C}{\partial z^2} + \lambda C - \frac{\phi D'}{(b/2)R}\frac{\partial C'}{\partial x}\right|_{x=\frac{b}{2}} = 0 \quad , \tag{21}$$

where z = coordinate along the fracture axis,
C' = concentration of solute in matrix,
D' = effective matrix diffusion coefficient, and
x = coordinate perpendicular to the fracture axis,
according to Tang, et al. With boundary conditions of:

$$C(0,t) = C_0$$
$$C(\infty,t) = 0$$
$$C(Z,0) = 0,$$

where C_0 is the source concentration and assuming longitudinal dispersion in the fracture is negligible, the solution [Tang et al. (1981)] is:

$$C/C_0 = 0 \qquad T < 0$$

$$C/C_0 = 1/2 \exp\left(-\frac{\lambda Rz}{V}\right)\left[\exp - \left(\frac{\lambda^{1/2} Rz}{VA}\right)\operatorname{erfc}\left(\frac{z}{2VAT'} - \lambda^{1/2}T'\right)\right.$$

$$\left. + \exp\left(\frac{\lambda^{1/2} Rz}{VA}\right)\operatorname{erfc}\left(\frac{z}{2VAT'} + \lambda^{1/2} T'\right)\right] \qquad T' > 0 \quad , \tag{22}$$

where: $T' = \left(t - \frac{Rz}{v}\right)^{1/2}$

and

$$A = \frac{(\frac{b}{2})\ R}{\phi (R'D')^{1/2}} \quad ,$$

where:

$$R' = 1 + \frac{\rho P}{\phi} K_d$$

and $D' = TD^*$,

where: T = matrix tortuosity

and D^* = molecular diffusion coefficient in water.

A porosity of 1% was assumed for the granite matrix. The other conditions and assumed parameter values for the estimate are:

Injection pressure = 3 psig,
V = 68 m/day,
K_a (for Sr) = 0.001 m^3/m^2,
K_d (for Sr) = 9 ml/g (lowest K_d value reported for Sr on Climax granite),
ρ = 2.65 g/cm^3,
T = 0.1,
D^* (for Sr) = 6.9 X 10^{-5} m^2/day, and
D^* (for ^3H) = 7.7 X 10^{-4} m^2/day.

The abrupt breakthrough of strontium shown in Fig. 10 is partly a relict of the form of the analytic solution of the transport equation. The actual strontium breakthrough would be expected to be somewhat more gradual. The strontium breakthrough time of about 43 h compares favorably with the time to the peak of the strontium pulse (54 h) given in Table 3 for the 20-μm fracture. Both tritium and strontium rise to near their input concentrations rapidly after breakthrough.

The main effect of matrix diffusion is to retard the arrival of reactive (and nonreactive) solutes beyond that predicted by simpler models of solute transport. The effects of matrix diffusion are obviously greatest in rock with substantial matrix porosity. The matrix porosity of the granitic rock

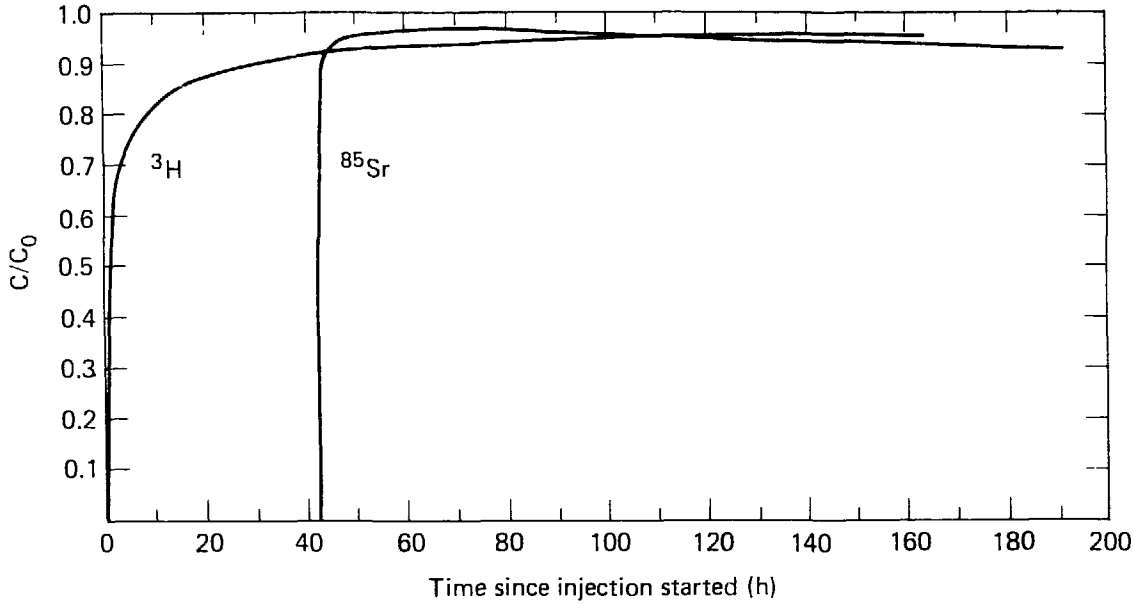

Figure 10. Breakthrough of tracers at outlet hole assuming constant-strength source and flow through 20-μm fracture. Longitudinal dispersion in fracture is neglected. Solutions after Tang et al. (1981).

of the Climax Stock is less than 1% [Maldonado (1977)], but there are systems of interconnecting fractures that lie just off the main water flow paths that may provide an equivalent matrix porosity. Lantz [Intera, personal communication (1981)] has concluded from a preliminary study of our hydraulic test data that matrix porosity may be affecting our results.

Simulation of the arrival of a tracer front resulting from a source of constant concentration is somewhat simpler than that of a finite pulse. Hence it may be prudent to consider a constant source tracer test. For the case of the 20-μm fracture with an injection rate of 1.2 ml/min or 1.7 X 10^{-3} m^3/day, one would need to inject approximately 0.01 m^3 or 10 litres of tracer solution to assure the breakthrough of tracers with retardation of the same magnitude or less than that of strontium. The basis for this estimate is the time needed to adequately study the strontium breakthrough curve for the 20-μm fracture given in Fig. 10.

4.3. DATA ANALYSIS AND INTERPRETATION

The results to be recorded are concentrations of various solutes in the flow from the outlet hole as a function of time. If simple models that do not involve matrix diffusion seem to describe the results, then the retardation coefficients can be calculated from the breakthrough or pulse peak arrival times of the tracers with the nonreactive tracer giving the average water travel speed. The surface distribution coefficient K_a can be calculated from a rearrangement of:

$$R = 1 + \frac{2\ K_a}{b} \quad , \tag{23}$$

where b is the effective fracture aperture width.

If the results indicate that matrix diffusion is important in influencing tracer travel times, a more sophisticated analysis is called for. A model such as that of Tang et al. (1981) will be used to arrive at estimates of the distribution coefficient in the fracture as well as that in the matrix. Estimates of the ground-water flow speed will initially be made based on hydraulic considerations and two retardation coefficients will be estimated, one for the matrix and one for the fracture. Successive calculations of breakthrough curves and adjusting parameter values as needed to match experimental results will be used to refine the initial ground-water flow speed and estimates of the distribution coefficient.

5. EQUIPMENT DESIGN AND OPERATION

This section describes the engineering design and operation of the equipment for the Radionuclide Migration (RNM) experiments. This design is based on criteria established from an evaluation of the state of the art in equipment development and on the results of the initial hydraulic testing of fractures. The system is divided into four distinct units: (1) the Packer System, (2) Injection System, (3) Collection System, and (4) Data Acquisition and Control System (DACS). Figure 11 shows the functional interaction of these units. The specific design criteria for each of the units are listed in Appendix I. The entire system must be safe from the standpoints of electrical and mechanical (pressure) failures and radionuclide contamination. In addition, the materials that come in contact with the radionuclides are required to be solid Teflon or Viton-coated steel to reduce sorption effects. This requirement, based on laboratory testing, may necessitate the modification of off-the-shelf equipment or the fabrication of equipment from original designs. Radionuclide (RN) sorption by the Teflon tubing walls over the approximately 30 to 50-ft lengths required will be tested.

5.1. PHYSICAL ARRANGEMENT

The apparatus will be built in modules that can be easily lowered down the shaft where they will be reassembled. The modular system, including two gas bottles, will be mounted on three detachable carts that have standard flanged railroad wheels to fit the existing rails in the drift. One cart will contain the DACS equipment and the other cart will contain the packer pressurization system and injection and collection systems. A smaller third cart will contain the waste tank and water supply and will be detachable from the larger carts.

The carts are made from high-strength welded aluminum plate with modular components bolted to the main frame plate. Figure 12 shows the physical system layout. The gas bottles are nested horizontally in the main frame of the hydraulics cart very low between the rails (low center of gravity for stability). The waste tank occupies a similar low position on its detachable cart to allow free gravity flow from the collection hole. The samplers are contained in dry-box enclosures in case of a malfunction or spill. All the

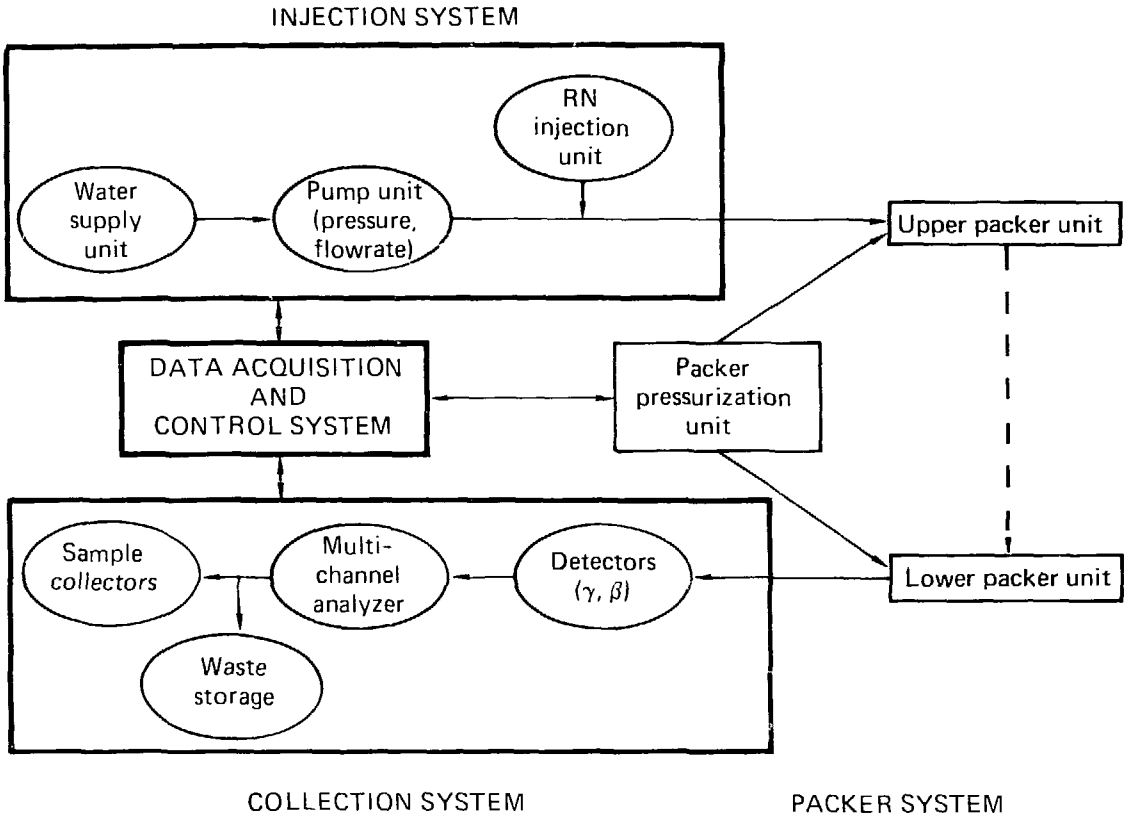

Figure 11. Functional interaction of equipment systems.

other systems will be appropriately protected from dust and moisture as required. Packer emplacement is manually controlled at the large cart and monitored at the DACS, which will be tied into the Spent Fuel Test Data Acquisition System (DAS) [Carlson, et al. (1980)]. Pump operations may be controlled from either the cart or the DACS as can the radiation measurement and sampling systems. Indicators showing system status are available at both the cart and DACS as well as in the DAS trailer on the surface. Interlocking prevents conflicting commands by allowing one or the other command point complete control at the operator's convenience.

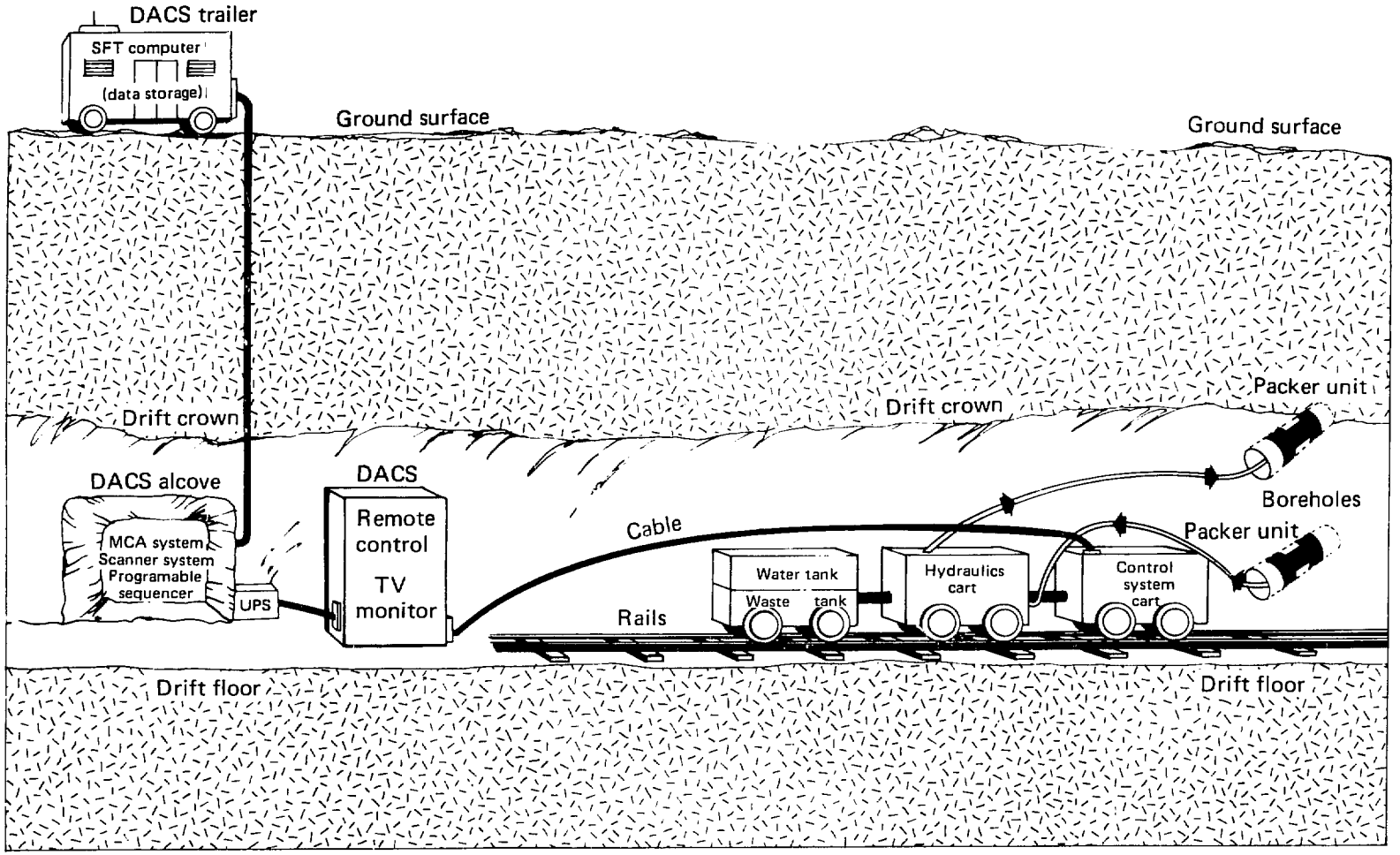

Figure 12. The physical system.

5.2. PACKER SYSTEM

The packer system includes a packer pressurization system and an upper and lower packer unit (Fig. 11). The packer units consist of a straddle packer with a center interval spacing that must permit adequate isolation of a single fracture. Access transmission tubes must be placed through the packer elements permitting monitoring of pressure changes in the packed off zone and the zone beyond the far packer, if needed during the experiment.

The packer units will be inserted into the boreholes and elements expanded tightly against the walls. The radionuclide tracers will be injected into the upper straddled interval and collected out of the bottom straddled interval. Since these intervals will be pressurized, the importance of the seals cannot be overemphasized from the standpoints of personnel safety and success of the experiments. The packer system plays a critical role in the experiment.

A variety of borehole packers are commercially available. However, previous experience has shown that leakage past packers is one of the most serious errors in hydraulic testing. Because of the design criteria (see Appendix I), only a few commercial companies could provide straddle packers for 76-mm (NX) boreholes that would be acceptable for modification. We found that the Cobbs packer, which is commercially available, has an advantage over balloon-type inflation packers in that the length of the straddled interval can be minimized.

The Cobbs packer design incorporates expandable rubber discs, which when compressed along their axis by a pneumatically or hydraulically generated force, grip the sides of a reasonably smooth borehole. The normal force (radial to the packer axis) seals watertight and generates a frictional force that resists axial movement of the packer. A straddle packer consists of two of these units mechanically connected together forming a small center interval as shown in Fig. 13. The packer requires fairly high pressure (up to 1500 psi) to ensure an effective seal.

Laboratory testing of the Cobbs packer revealed a magnitude of leakage past the sliding seals that precluded using pneumatic inflation. The leakage was reduced, although not eliminated, by switching to water as the pressurizing medium. An analysis of the Cobbs packer design according to LLNL standards gives it a maximum manned-area rating of only 800 psi. This results

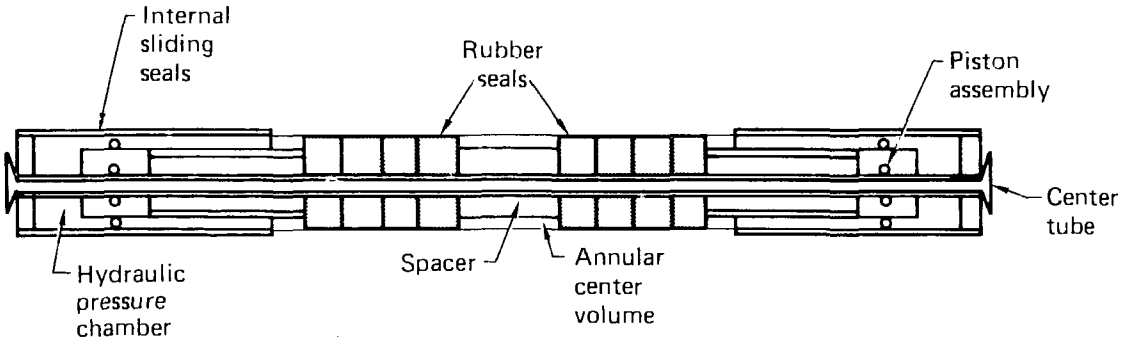

Figure 13. Cobbs style straddle packer unit.

primarily from lack of material and welder certifications and no evidence of quality-control inspections. In spite of these difficulties, LLNL acceptable practice allows use of such equipment with mechanical barricades over the boreholes and previous pressure testing to 1.5 times the working pressure. These precautions take care of the shrapnel danger. However, they do not address radionuclide leakage and subsequent contamination hazard to personnel.

We examined the possibility of reworking the commercial unit to eliminate all the possible problems we could find. The problems and necessary design and fabrication changes are summarized in Table 4. The difference in cost between reworking the commercial unit and fabricating our own packer consisted of a small amount of material and some drafting time. We chose the latter and have redesigned the original Cobbs packer. The result will be a certifiable, manned-area qualified packer system capable of withstanding full gas bottle pressure in case of regulator failure. This design includes materials (i.e., Teflon and Viton) that will minimize radionuclide sorption on the equipment.

We plan to use hydraulic actuation of the packer for minimum leakage by using the system shown in Fig. 14. The water reservoir vessels are weighed by load cells and monitored at the DACS. This provides a leak rate measurement and, along with the pressure measurement, alerts the DACS interlock system to take action if leak rates become significant. This approach also provides a power independent pressure supply that can be maintained at pressure in spite of volumetric changes in the high-pressure plastic lines supplying the packers. The lines are plastic because of flexibility requirements and are physically protected in flexible conduit.

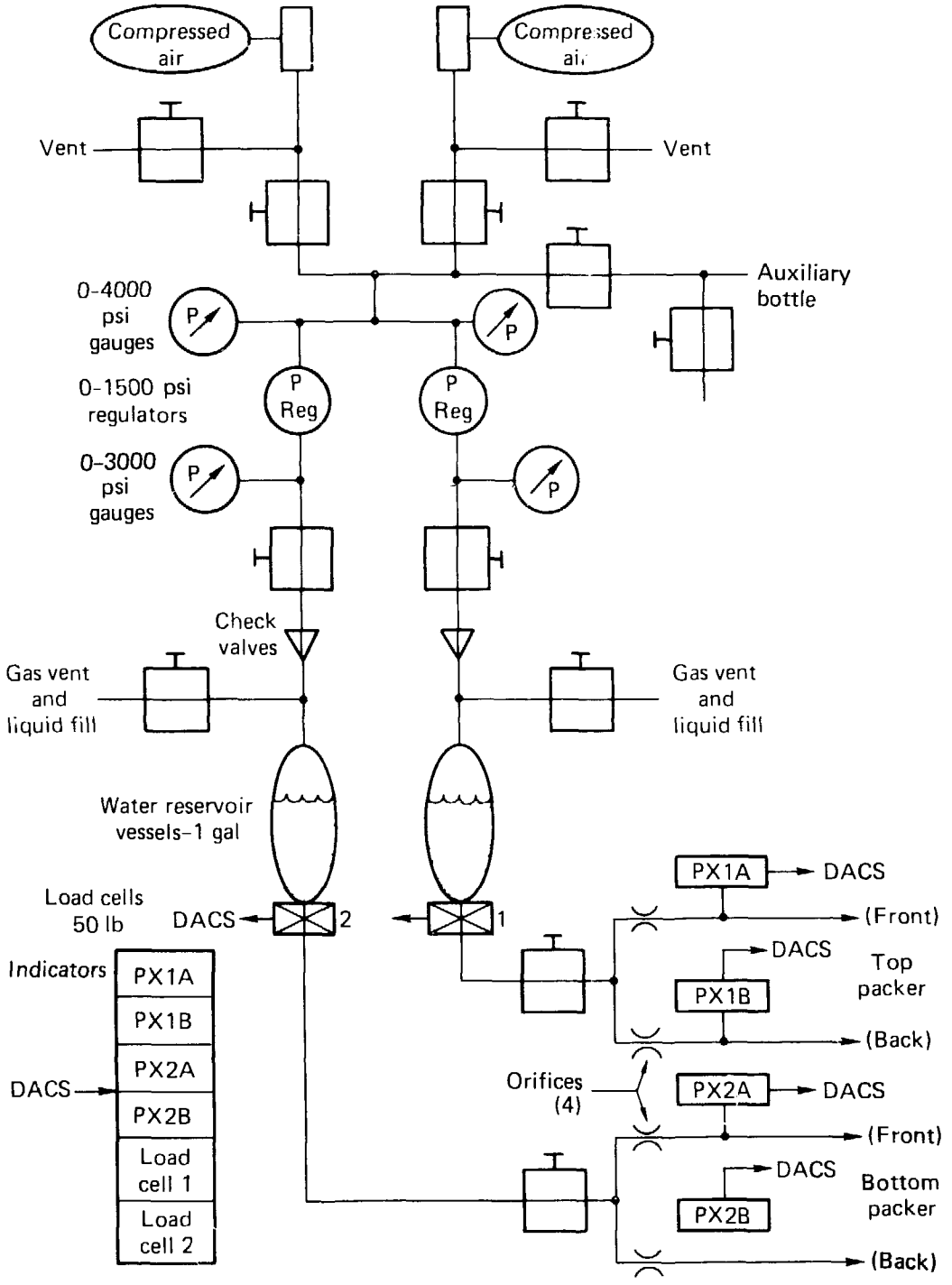

Figure 14. Packer pressurization unit.

Table 4. Analysis of Cobbs packer.

Fabrication/manufacturing problem	LLNL design correction
• Lack of certification of materials and processes imposed a low limit on allowable manned-area pressure capability (800 psi).	Specified LLNL-purchased certified materials for vendor fabrication, required welder certification, quality-control inspection, and proof testing.
• Minimal wall thicknesses, particularly in the center tube threaded and slotted areas, for manufacturer's pressure rating (the slots provided passageways to inflate a second packer).	Increased section sizes to next larger standard sizes for the cylinders and center tubing. Removed the slots. Tubing will be inserted through the center tube to inflate the second packer.
• Cylinder circumferential weld-placement created crevice for corrosion attack.	Moved circumferential weld down the cylinder. Eliminated crevice.
• O-ring grooves not sized for rolling action, roughly finished, contributed to seal leakage.	Sized grooves for rolling action, tightened dimensional tolerances of grooves, and specified surface finish.
• Peeling nickel plating.	Specified appropriate finishes for all areas, from hard chrome plating to paint.
• Rough threads, oversized holes contributed to sealing problem.	Tightened tolerances.
• Rubbers could not be changed without disassembly of piston-cylinder seals with high danger of seal damage.	Rubbers can be changed from the other end without disturbing the piston-cylinder-seals assembly. Threaded connection substituted for welded end-piece.

We plan to thoroughly test the redesigned packer in the laboratory to determine frictional holding power as a function of piston pressure. Leak rates of the hydraulic cylinder seals and the center volume seals will be measured also as a function of pressure in their respective volumes. Figure 15 shows the experimental test apparatus we plan to use. Although we can simulate certain conditions of use, some of the unknowns involved are the frictional characteristics of a given borehole in the granite including natural water

Table 5. Packer system measurement requirements.

Location	Measurement function[a]	Type of transducer	Range	Accuracy (±%)
Gas bottles	Pressure	Bourdon gauge	0 to 4000 psi	1
Regulators	Pressure	Bourdon gauge	0 to 3000 psi	1
Water vessels' load cells	Force	Strain gauge	0 to 50 lb	2
Packers	Pressure (PX1A and PX2A) (PX1B and PX2B)	Strain gauge	0 to 3000 psi	1

[a] Numbers in parentheses identify location of transducer in Fig. 14.

lubrication of the rubbers. Higher cylinder pressure may be required to effect an acceptable radionuclide seal under this latter condition.

Table 5 summarizes the measurement requirements for the complete packer system. Calibration of pressure transducers and load cells will be done by the LLNL calibration laboratory using NBS derived standards. Flow calibration will be done in our laboratory and will be based on mass per unit time measurements with calibrated weight and timing apparatus. The use of bourdon gauges for gas bottle and regulated pressure is standard practice. The pressure transducers and the load cells were chosen for reasons of remote sensing, stability, and availability.

5.3. INJECTION SYSTEM

Natural granitic ground water collected from seeps in the Piledriver drift will be used for the experiment. The water will be pumped through an ultrafilter into the system reservoir, a 55-gal polyethylene container (Fig. 16). This will ensure removal of suspended particulates down to $<0.002\ \mu m$ and should minimize problems associated with injectivity and fracture plugging. Water flows from the reservoir through a check valve and is pumped by one or more of three small gear pumps driven by dc motors (Fig. 17).

The pump capacities were based on required flow rates and pressure. Figure 18 shows that the size of the aperture width determines the flow rate at a

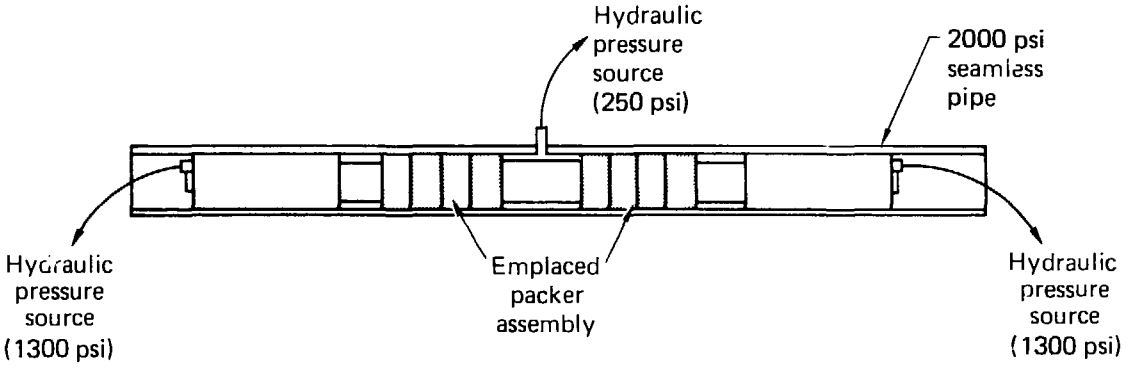

Figure 15. Borehole simulator for laboratory packer test.

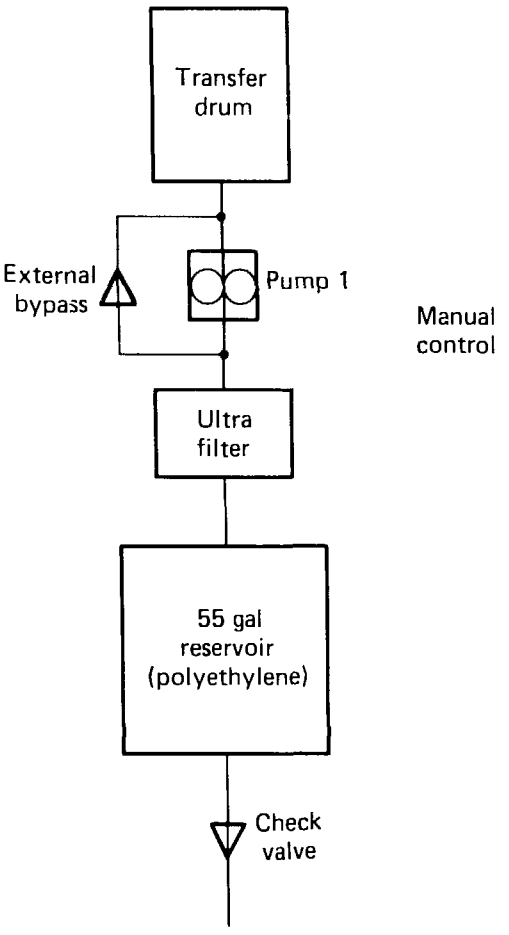

Figure 16. Water-supply unit.

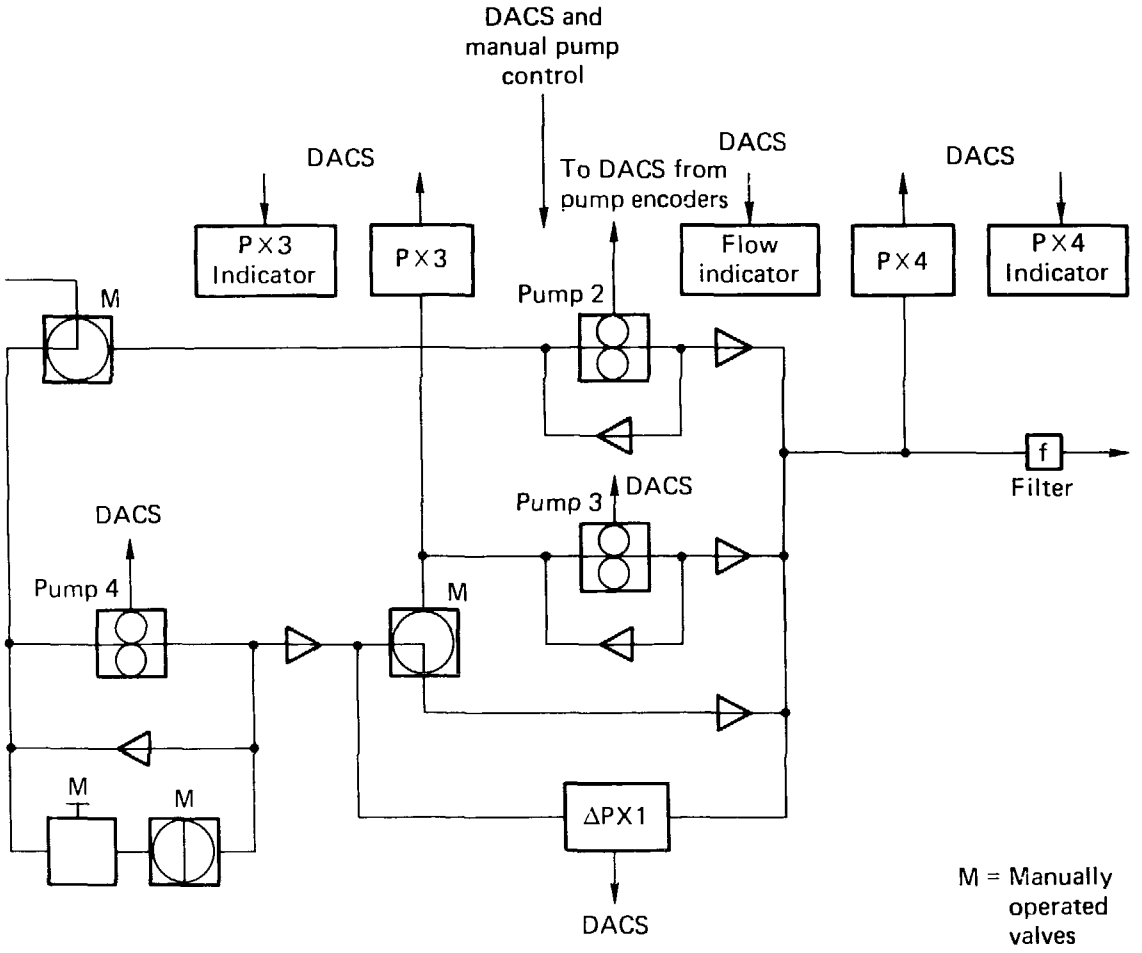

Figure 17. Injection-pump unit.

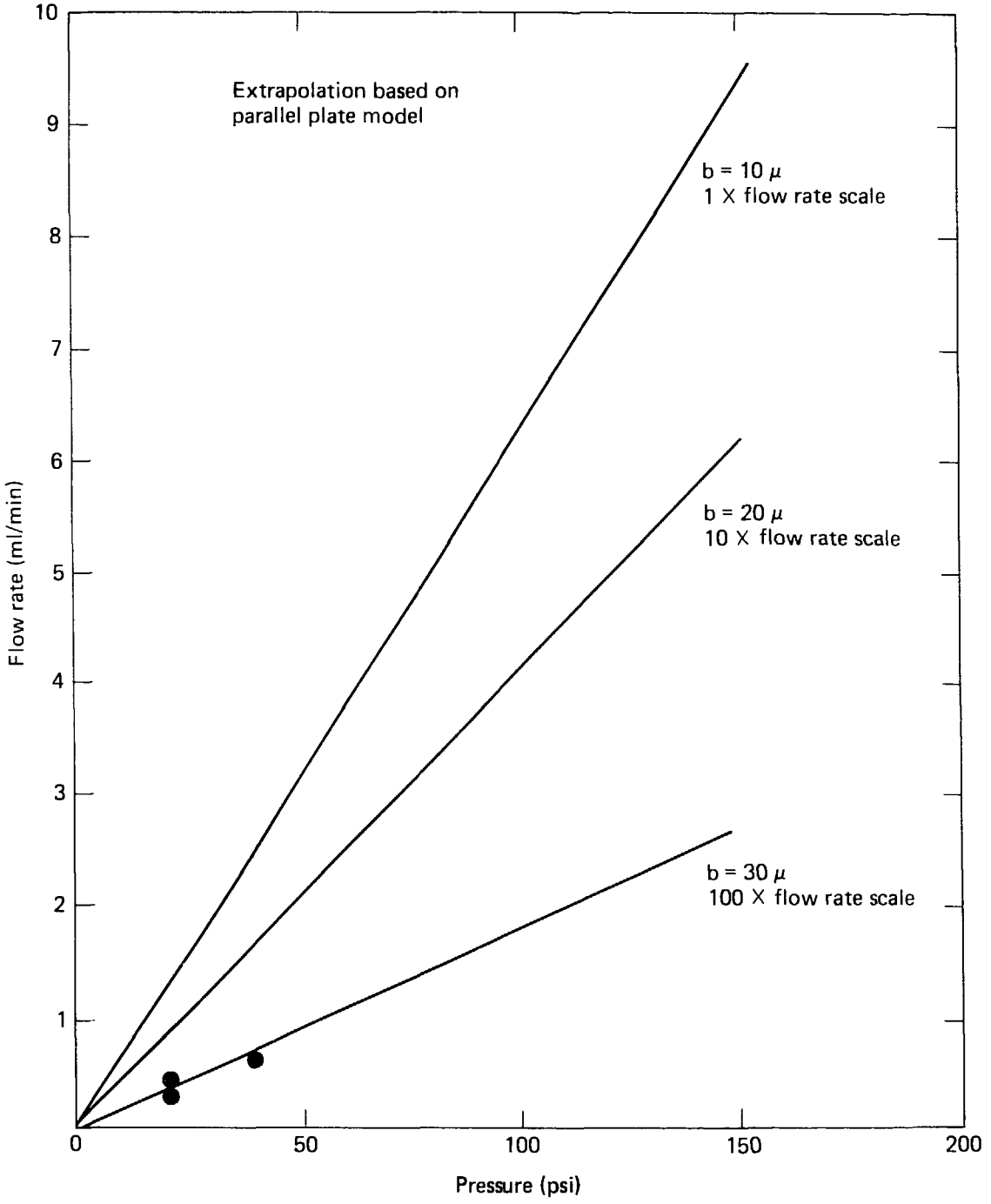

Figure 18. Flow rates vs pressure for three aperture widths (• = data from initial hydraulic testing). Extrapolation based on parallel-plate model.

given driving pressure. For example, the smallest pump rapidly becomes pressure limited (40 psi) for a 10-μm aperture and this pressure limit establishes a flow limit of about 2.6 ml/min. For a 20-μm aperture the same pump becomes flow limited at 6 ml/min with a corresponding pressure limit of about 11 psi. To provide the higher pressures (and flows) required for a 10-μm aperture, we arrange the larger pump to boost the input pressure to the smaller pumps. All the pumps are capable of withstanding 600-psi system pressure. This pump combination provides the flexibility to produce 0.25 to 9-ml/min flow rates in a 10-μm aperture, 0.25 to 60-ml/min flow rates in a 20-μm aperture, and 0.25 to 240-ml/min flow rates in a 30-μm aperture.

The control system allows only one pump or pump combination to be operational at a time. The largest pump is intended for fast fill of the system and is capable of 8 to 630 ml/min up to 175-psi maximum pressure. It also boosts the input (and output) pressure capabilities of the small pumps. The smallest pump operates from 0.25 to 6 ml/min up to a maximum differential pressure of 40 psi. The third pump covers the 1.5 to 30-ml/min range up to a maximum differential pressure of 45 psi. This third pump serves to complete the coverage as well as to back up the other pumps. Since these are gear pumps, overpressure bypass valves are provided. These pumps are also magnetically coupled and will decouple under overload. The pump outputs are protected against possible reverse flows by mechanical check valves. The input and output pressures will be monitored and the effluent filtered to remove particulates introduced by pump wear. The reservoir is positioned to keep the pump gears wetted at all times. Flow measurement is accomplished by encoders on the pump motors that furnish a measure of pump volume, which yields volumetric flow when coupled with the pressure measurement. The use of encoders on the pump motors rather than conventional flowmeters stems from the exceptionally low-level flow requirements. This flow indication is returned from the DACS unit to a digital readout on the cart as are all pressure transducer readings. Table 6 summarizes the injection system measurement requirements. There will be a choice of constant flow or constant pressure control provided by the DACS.

The metered flow bypasses the tubing coil containing the radionuclides and fills the packed-off volume from the bottom up to expel the residual air through the pressure tap tubing at the top. This flow is vented to the waste container. When the system is saturated (filled), the desired flow rate or

Table 6. Injection system measurement requirements.

Location[a]	Measurement function[a]	Transducer	Range	Accuracy (±%)
Pump input	Pressure (PX3)	Strain gauge	0 to 300 psia	1
Pump output	Pressure (PX4)	Strain gauge	0 to 300 psia	1
Center volume	Pressure (PX5)	Strain gauge	0 to 300 psia	0.5
Trapped volume	Pressure (PX6)	Strain gauge	0 to 300 psia	1
Pump (2)	Flow	Encoder	0.25 to 6 ml/min	1
Pump (3)	Flow	Encoder	1.5 to 30 ml/min	1
Pump (4)	Flow	Encoder	8.4 to 630 ml/min	1
Differential pump	Pressure (ΔPX1)	Variable reluctance or strain gauge	0 to 50 psid	1

[a] Numbers in parentheses identify locations in Figs. 17 and 19.

pressure may be established by the DACS. The volume trapped behind the packer in the blind hole may be monitored for pressure buildup (leaks from center volume or packer piston).

The radionuclide injection system shown in Fig. 19 is controlled by a series of valves to allow the 10-ml sample to be integrally injected at normal flow rate speed or as a continuous dilution in the main flow. The radionuclides are preloaded in a valved tubing coil that is connected to the system for injection. For integral injection at normal flow rates the flow is diverted through the sample coil. The precise time the sample enters the central volume may be calculated from flow rate data. At this point the 10-ml pulse-injected sample is diluted by approximately 90 ml of water in the central volume. The sample may also be introduced into the main flow as a very slow continuous dilution by use of a bypass metering orifice. In all cases the sample is forced through an orifice as it enters the central volume to enhance velocity and promote mixing. Then the diluted radionuclide solution enters the rock fracture and flows in the established pattern to the collection interval in the lower borehole. Calibration experiments are planned using a simulated borehole to test whether a linear mixing of tracer fluid occurs in the central volume and to quantify the dilution effects. If linear mixing does not occur, then the tracer input history will need to be adjusted based on the calibration data.

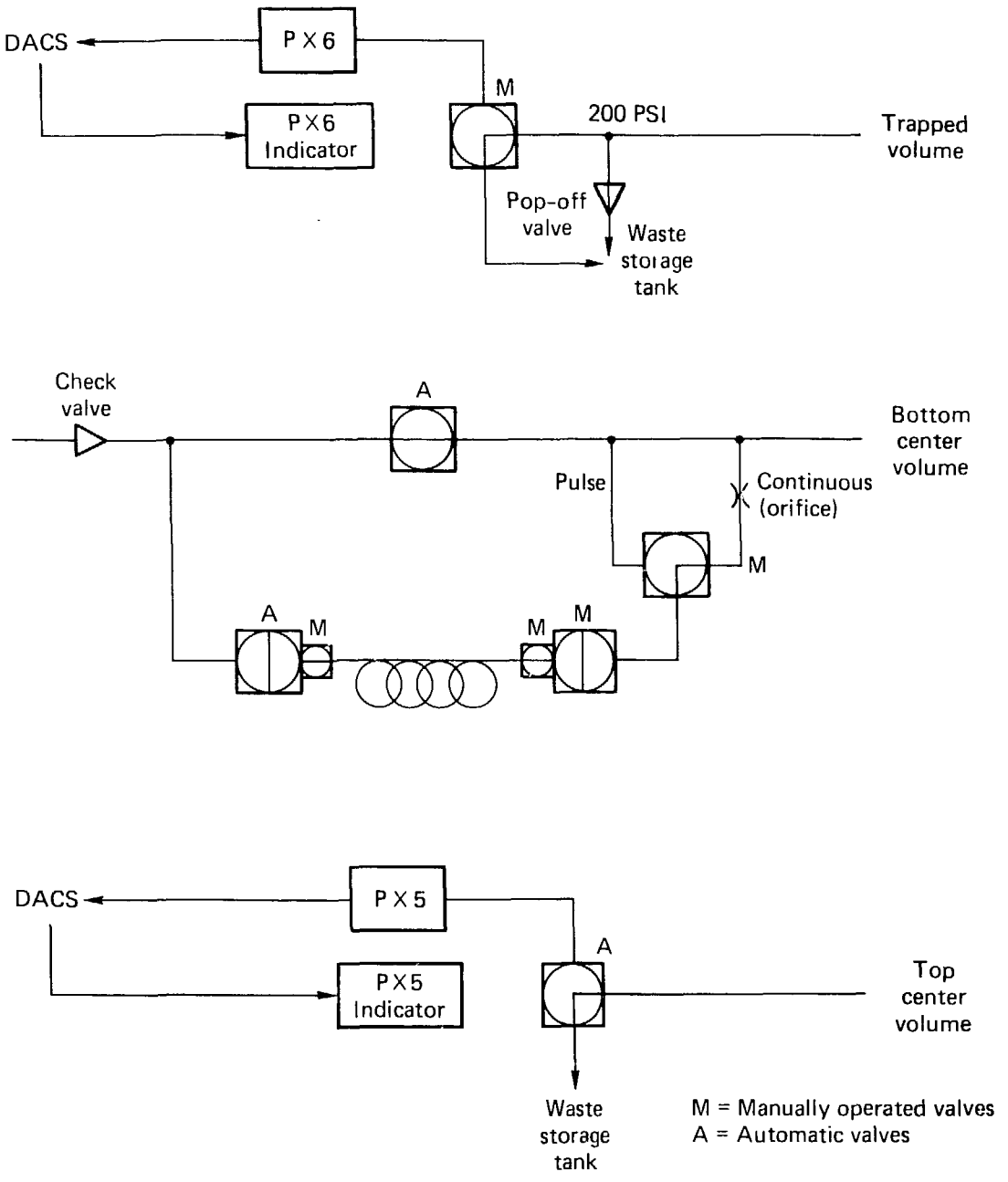

Figure 19. Pulse and continuous radionuclide injection unit.

5.4. COLLECTION SYSTEM

Figure 20 shows the general schematic for both the injection and collection systems. The two systems are tied together by the natural fracture. The collection packer unit is almost identical to the injection packer except for two significant differences. First, the collection packer annulus or center cavity is maintained at atmospheric pressure. Since there is no internal pressure to contain, leak-free sealing in the lower borehole is somewhat easier. The blind-hole volume will be monitored for pressure buildup (leaks from the packer piston or a fracture interconnected with the injection hole).

Second, the straddled interval is kept at approximately a level equal to a 12-ml volume using a pump controlled by a proximity probe in the interval. This improves the time resolution of radionuclide arrivals by placing the tracer solution into the 1.6-mm Teflon line immediately upon arrival, minimizing dilution and sample overlap. The flow control is accomplished by the same method as the flow input by using positive displacement pumps. Figure 21 shows the collection system schematic. Table 7 summarizes measurement requirements for the system.

All collected fluid flows through the β^- and γ detectors and depending on the activity level is directed by the DACS to the samplers or to waste storage. The fluid will initially be seen by a NaI (Tl) crystal (7.62 X 7.62 cm) for gamma detection. The tracer solution will pass through tubing coiled across the face of the crystal such that the detector sees 3 to 5 ml of the sample. The sample will then go into an electronic stream splitter/mixer where a fraction of the fluid will be mixed with a liquid scintillator and be counted by the beta detector (scintillation counter). The fluid mixed with the scintillator will then go to waste storage.

The other portion of fluid that was split off before mixing will go to the sample collectors. Two 400-tube samplers allow alternately valving one or the other on-line. The off-line sampler may have its magazine of sample tubes replaced at any time allowing unlimited sampling capability. Sample tubes are identified by bar code and arabic numerals. Their identity and fill time is recorded by the DACS. The samples will be collected at preset sampling times that can be changed manually during the experiment. This may

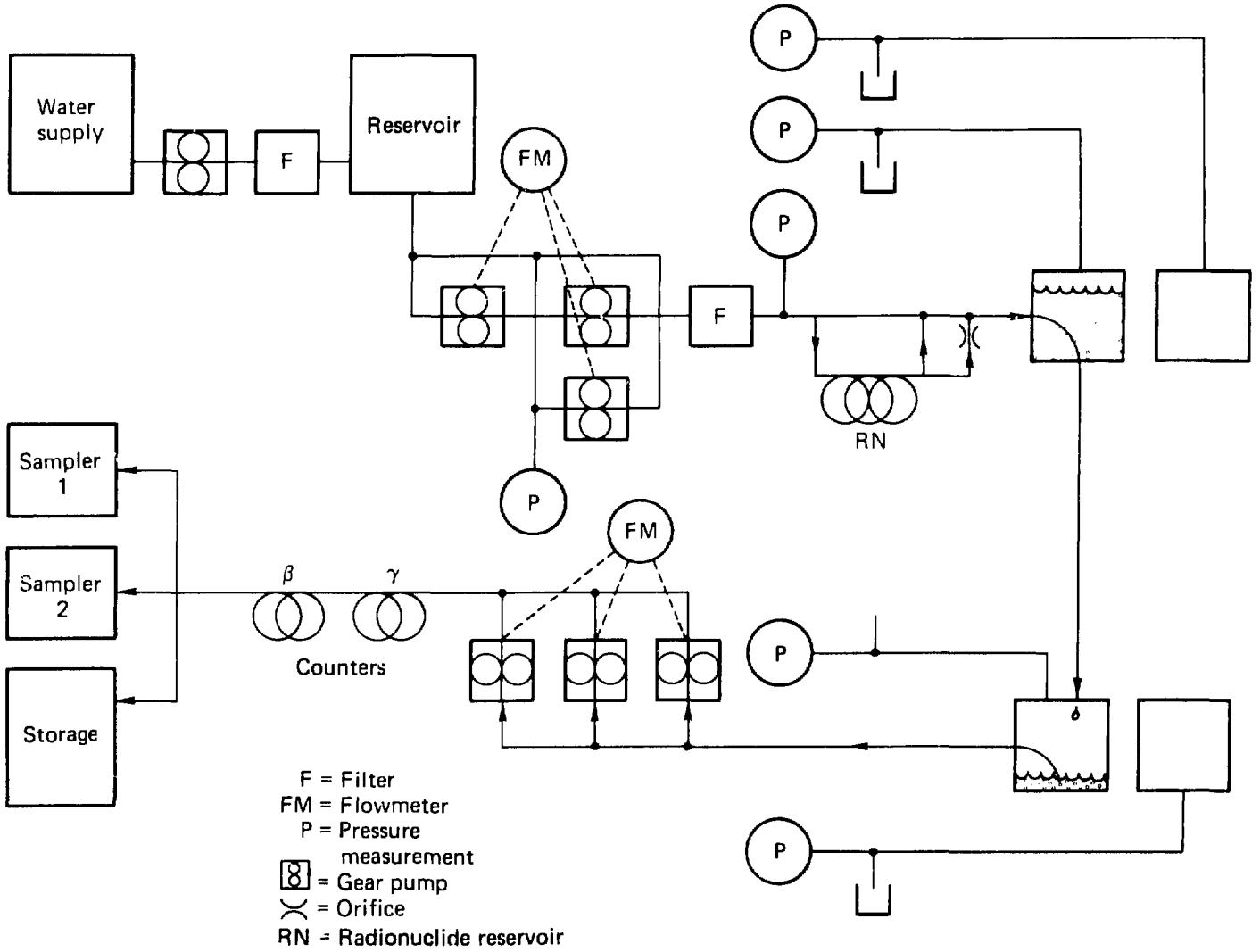

Figure 20. Schematic of injection--collection system.

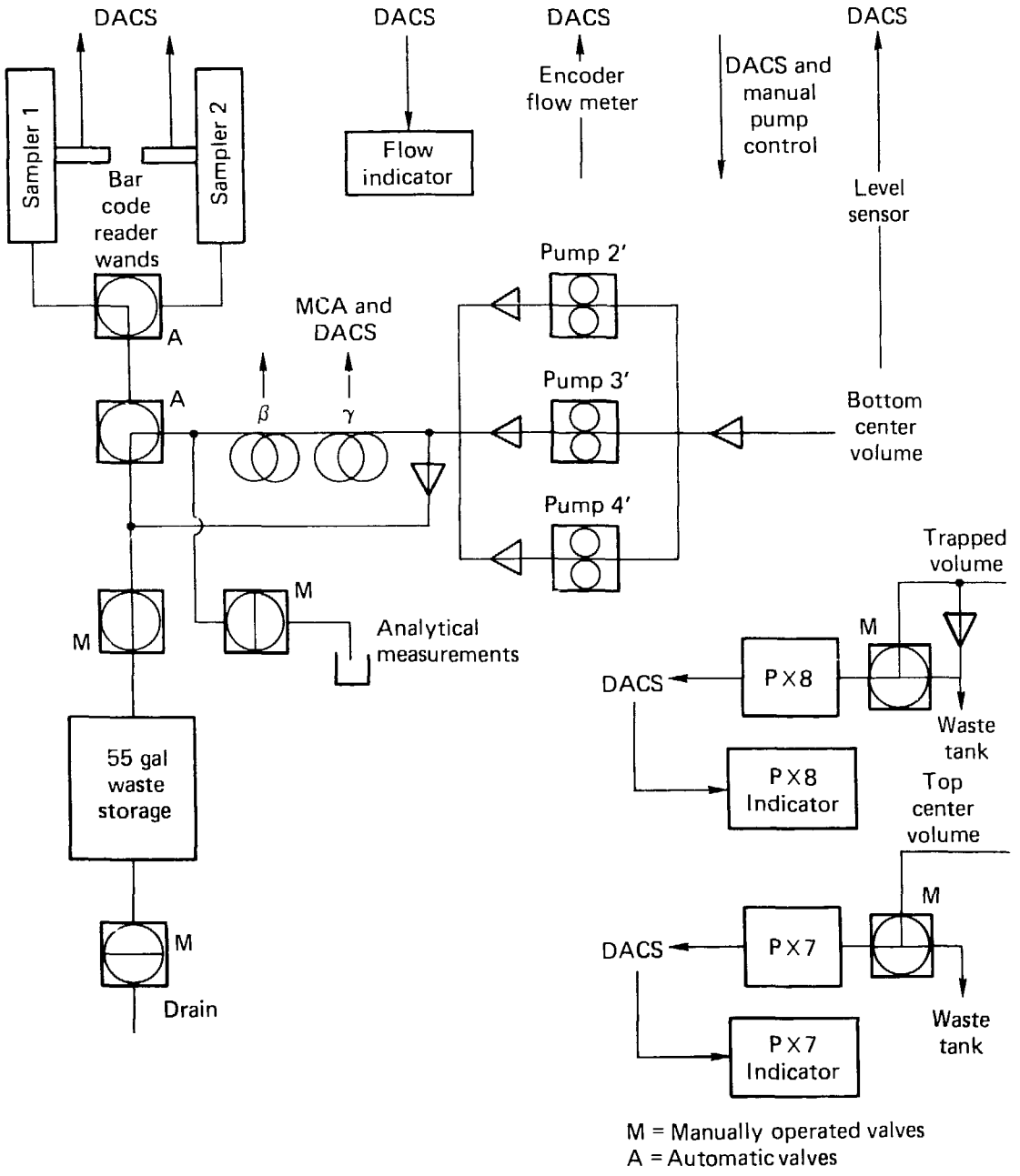

Figure 21. Collection system schematic.

Table 7. Collection system measurement requirements.

Location[a]	Measurement function[a]	Transducer	Range	Accuracy (±%)
Center volume	Pressure (PX7)	Strain gauge	0 to 25 psia	0.5
Trapped volume	Pressure (PX8)	Strain gauge	0 to 25 psia	1
Pump output	Pressure (PX9)	Strain gauge	0 to 300 psia	1
Pump (2')	Flow	Encoder	0.25 to 6 ml/min	1
Pump (3')	Flow	Encoder	1.5 to 30 ml/min	1
Pump (4')	Flow	Encoder	8.4 to 630 ml/min	1

[a] Numbers in parenthesis identify location in Fig. 21.

be necessary after establishing breakthrough times. The output from the β^- and γ detectors will be routed to an on-line multichannel analyzer. This will be hooked to the DACS for graphics display and data reduction and storage.

5.5. DATA ACQUISITION AND CONTROL SYSTEM (DACS)

To take advantage of existing hardware and software, the RNM data acquisition and control will be an expansion of the Spent Fuel Test (SFT) DACS. The interaction of these systems can be seen in Figs. 12 and 22. This has several advantages:

- Computer redundancy.
- Computational and graphics capabilities.
- Alarm systems, local and remote.
- Remote monitoring of the experimental parameters.
- Remote control of experiment.
- Existing software applies directly.

The DACS will be contained in a temperature, humidity, and dust controlled area. The SFT EE alcove meets these requirements. The control systems can be remotely operated from this location. Utility power has already been provided

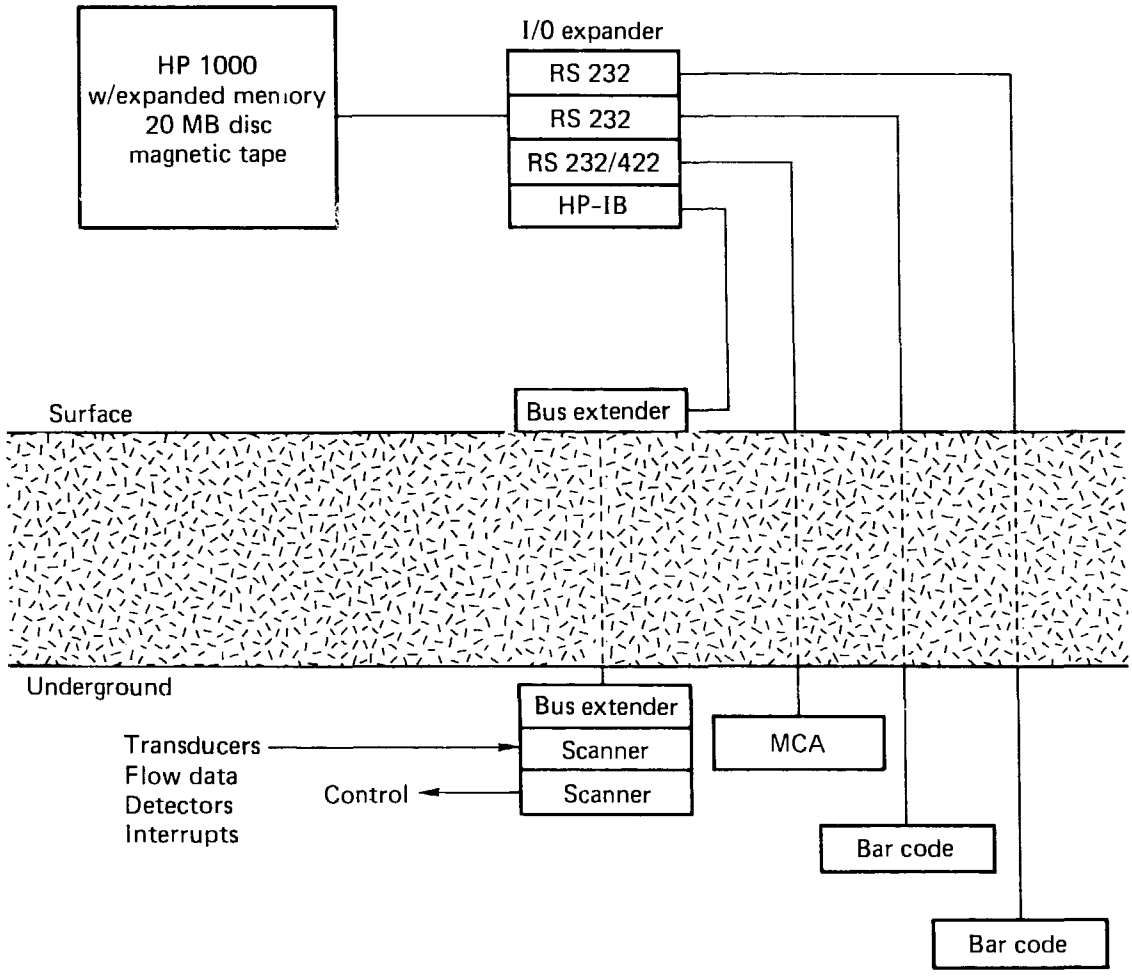

Figure 22. Data acquisition control system.

as a portable multioutlet box in the experimental area. Instrument power will be provided by the existing SFT uninterruptible power supply (UPS). The only modification to this system will be in the form of additional batteries to maintain power for 4 h as per the design criteria in Appendix I.

Data Acquistion

The experimental data will be fed into an incremental scanner system. The DACS will scan individual channels at a predetermined rate. The raw data values will be converted to equivalent engineering values and displayed on a monitor adjacent to the control panel. The data are examined to determine if they reside between two limit values. If they are between these limits, the data are put into memory. If they are out of limits, the alarm processor will initiate either a corrective action and/or an alarm to a specified location (i.e., CP40, DAS TRAILER, LLNL).

The DACS will include an interrupt feature that allows instantaneous reaction time to system malfunctions such as packer failure or failure of the injection pumps. The interaction with the control system is accomplished by a relay output module interface.

The DACS will provide a computed flow rate output to be displayed on the control consoles in engineering units (cm^3/min). This will be accomplished by converting a digital number to an analog voltage at the scanner interface. The voltage can be interpreted as a flow rate (e.g., 1.00 V = 1.00 cm^3/min).

On-line flow through β^- and γ detectors will monitor the outlet fluids for radionuclide activity. The β^- and γ detector activity will be recorded as an analog voltage and interpreted automatically by a calibration curve in the DACS database. The levels will be visible on a TV monitor adjacent to the control consoles. The β^- and γ detector output will be fed into a multichannel analyzer (MCA). The output of the MCA, which is controlled by an LSI-11 microprocessor, will be interfaced to the DACS computer to provide storage on magnetic tape. Output from the MCA will be available on hard copy to follow the progress of the experiment.

Control System

Because of the complexity of the control logic and the need for flexibility, a microprocessor-controlled programmable sequencer (PS) will be the design base for the control system (Fig. 23). The PS will make the logical decisions based on Boolean expressions programmed previously and output necessary signals to operate the solenoid valves in the system. The memory in

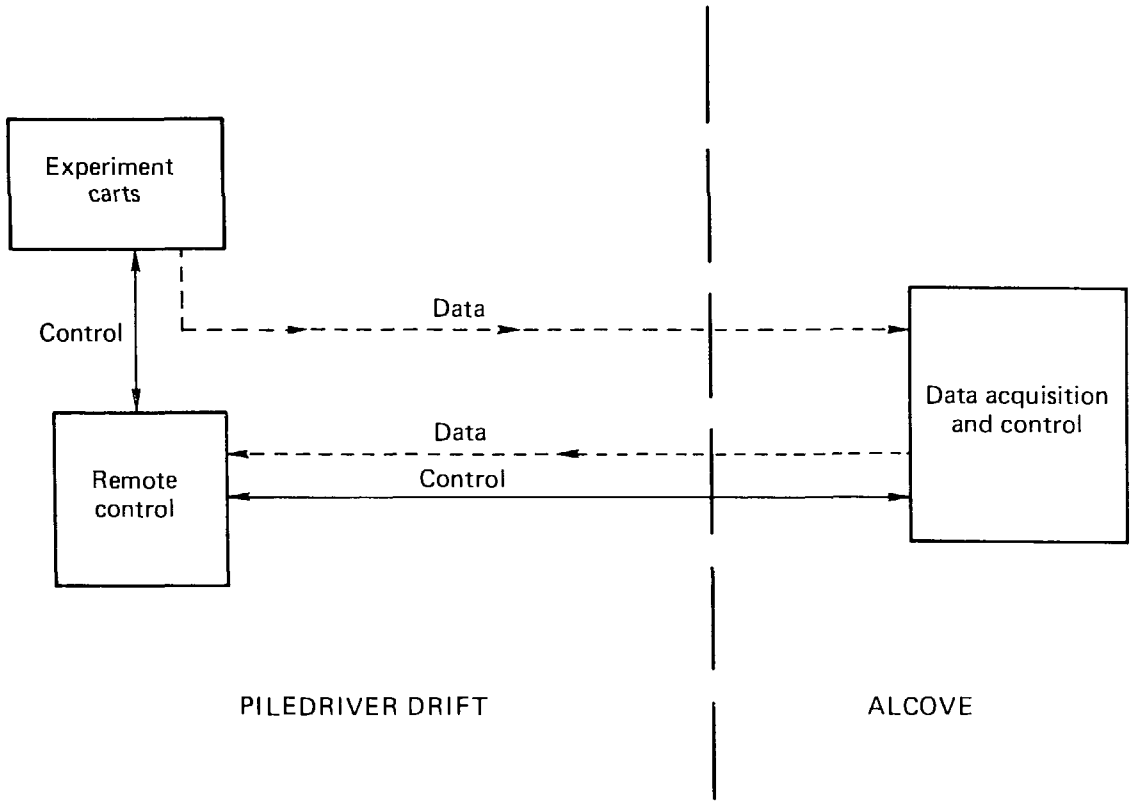

Figure 23. DACS control system.

the PS is a nonvolatile programmable read only memory (PROM). If for any reason a particular sequence of operations is changed, the program can be easily altered.

An interlock system programmed into the PS will allow only one control panel to be in control at any one moment. A key will be necessary to activate any function on either panel or to transfer control to the remote panel. In case of a power failure the system will recover in a safe mode.

Injection System Controls

The experimental fluid flow rate will be controlled by a commercially available process loop controller (L/C). The volumetric gear pumps will monitor motor speed by an encoder mounted on its drive shaft (Fig. 24). An ideal gear pump delivers a constant flow rate at a constant motor speed

regardless of the output line pressure. Since this is not an ideal case, we will monitor the output line pressure to provide the necessary correction factors for a true flow rate. This will be done with:

$$\text{Motor speed X f(line pressure)} = \text{flow rate} \quad . \tag{24}$$

Either the computed flow rate or the line pressure may be fed into the loop controller to provide the process variable. A remotely entered set point (from either control panel) will set the flow rate and control the pump motor speed.

In case of equipment failure (e.g., power supplies, loop controller, etc.), the experimental control system as well as the computer will be monitoring the line pressure and flow rate and can shut the system down. In case of a power failure, the pumps will shut down and will have to be manually restarted. This can be done remotely if necessary.

Collection System Controls

The collection flow rate system will be similar to the input except that it will be controlled by a proximity detector located in the center volume of the collection straddle packer (Fig. 25). The loop controller (L/C) will be adjusted to maintain a constant level in the collection volume. A constant input flow rate should yield a constant output flow rate, assuming steady-state conditions are reached.

The collection system will be controlled by a time-volume priority system (Fig. 26). If the predetermined time interval has been met or the fluid level in the collection volume exceeds a given preset level, the sampler will increment. Each time a new sample is begun, a bar-code reader will scan the sample volume and enter into the database the sample number, time, and date.

5.6. EXPERIMENTAL OPERATIONS

The first task is to locate a potential fracture connecting the upper and lower boreholes. This is done by visual logging with a high-resolution borescope. The borescope has scribed divisions along its length to allow accurate fracture location and subsequent emplacement of the straddle packer.

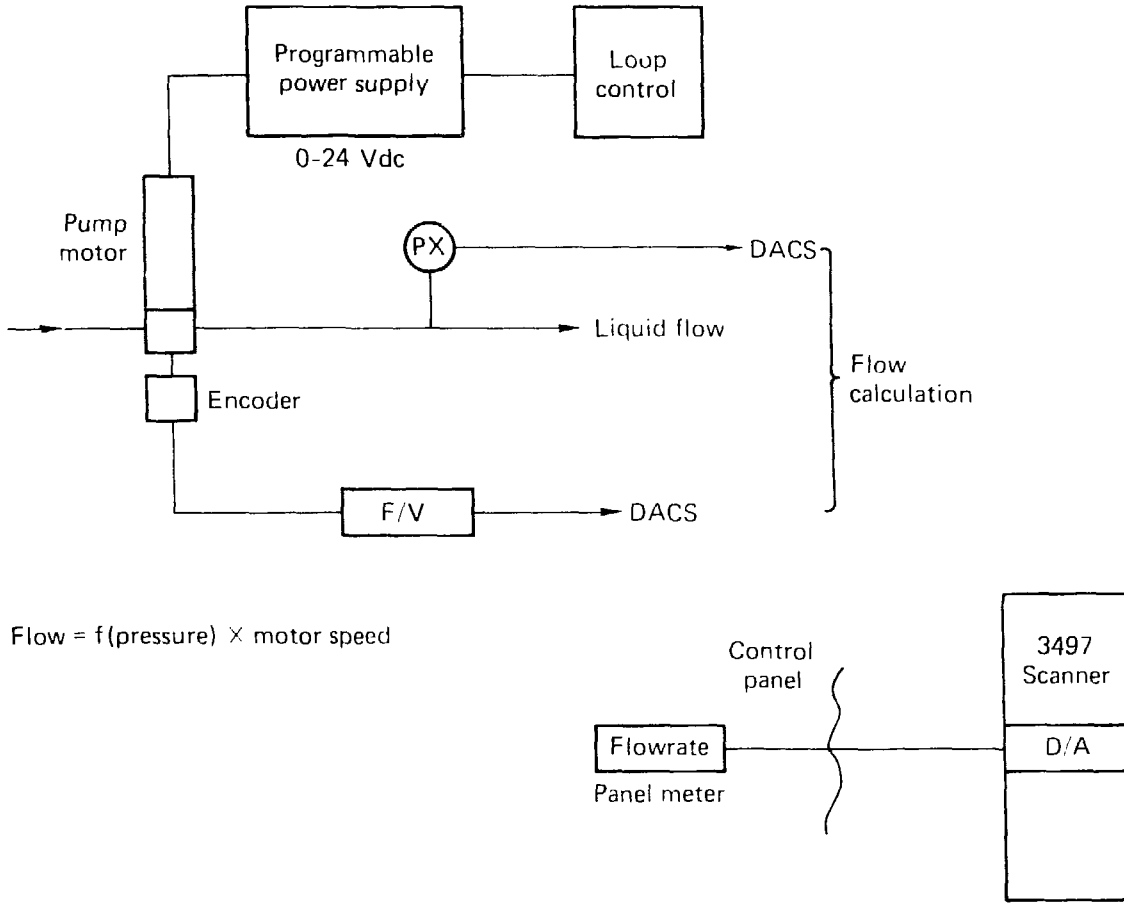

Figure 24. Flow control and indication (input); F/V = frequency to voltage convertor.

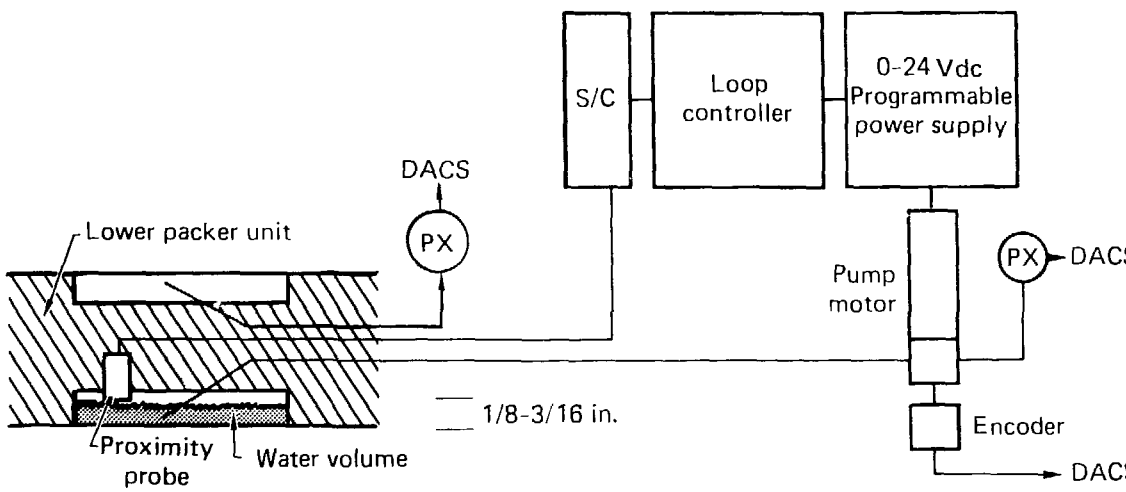

Figure 25. Flow control and indication (output).

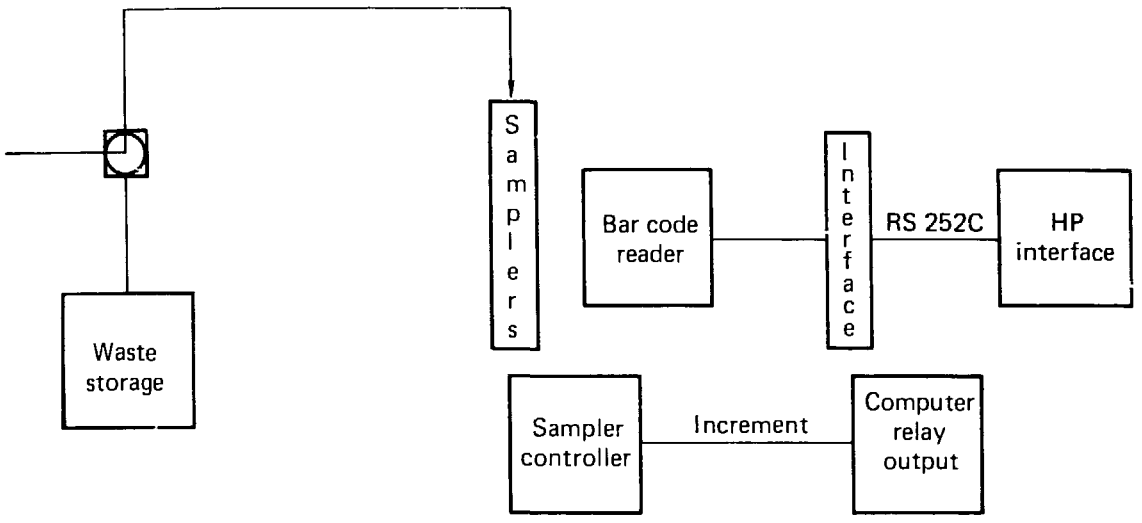

Figure 26. Collection system controls.

The next step is emplacement of the top packer and saturation of the fracture. When the interconnecting fracture in the bottom borehole can be identified visually using the borescope to determine which fracture is dripping water, the bottom packer assembly is installed to establish a circulating flow system between the two boreholes. The particular fracture characteristics can then be analyzed by conducting flow and pressure tests. If the fracture characteristics are acceptable, the migration test begins. If not, the procedure is repeated until an acceptable fracture is located. Whether a fracture is acceptable or not will be determined by interpreting the hydraulic test data using an appropriate model.

All operations to this point are conducted at the cart location immediately adjacent to the boreholes. All operations are manually performed such as valve operation, packer emplacement and inflation, etc.

Once a suitable fracture is chosen and a steady-state circulating flow system is established, the radionuclides are loaded into the injection equipment. The injection equipment is pretested with water to ensure correct operation. At this point the personnel retreat to the remote DACS location after checking system interactions and functions such as the collection pumps and samplers. All reservoirs and gas bottles are also checked for adequate levels. With the systems operational, the injection command is given to the

DACS. Injection verification may be obtained from the radiation monitor at the entrance to the top borehole. Exact injection time is calculated from the flow rate and the injection command time.

Assuming no problems, the DACS takes over operations for the test period. Certain manual operations may be performed at the cart during the test period such as drawing samples for chemical tests (pH, etc.). Sampling rates may be manually changed during the test period. Access to data can be obtained during the entire test period from the DACS.

When the test is complete, the system is shut down by turning the pump(s) off. The injection and collection volumes are flushed to the waste tank and residual fluid gravity-drained to the waste tank.

The packers are deflated one at a time and carefully removed, monitoring for residual radioactivity. Removal into plastic bags as shown in Fig. 27 is done as a precaution. The tubing is disconnected at the cart and bagged and the emplacement pipe is bagged and taped. These components are then transported to a decontamination facility. The boreholes will be sealed with commerically available rubber pipe plugs and labeled with appropriate warnings. The waste tank is decoupled from the main cart and rolled down the track to the elevator where it is removed and transported to on-site disposal facilities. The sampler magazines are removed and transported to LLNL for analysis. The remainder of the system is inspected and monitored for radioactivity. Necessary clean-up follows. An area survey completes the search for inadvertent radionuclide loss.

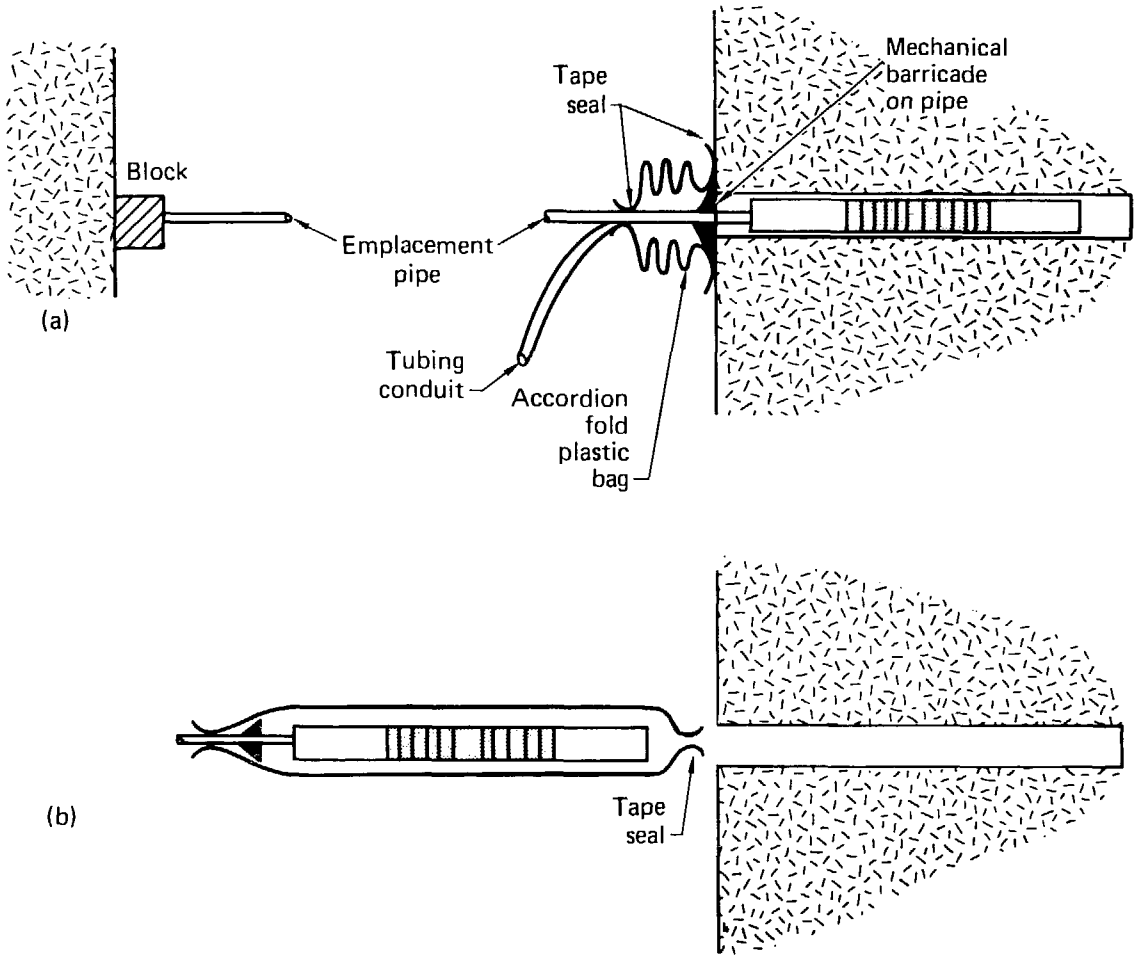

Figure 27. Packer removal.

6. SAFETY ASPECTS

A safety analysis and review process will be performed prior to the initiation of the RNM experiments. A Safety Assessment Document (SAD) will be issued in compliance with DOE requirements. The SAD will evaluate and determine that:

- Potential hazards are systematically identified.
- Potential impacts are analyzed.
- Reasonable measures to eliminate, control, or mitigate the hazards have been taken.
- There is documented management authorization of the operation based on an objective assessment of the adequacy of the safety assessment.

The following is a brief summary of the safety procedures in the event of a system failure.

It is necessary to monitor both borehole openings for radionuclide activity to discover any leakage problems early in the test period. This system, plus an area monitor to detect system failure or leakage, will be integrated with the Spent Fuel Test alarm system. This is shown in Fig. 28. In addition, two closed-circuit TV systems are planned to monitor the general area and may be manually positioned to observe specific areas of interest. Emergency shut-off switches will be installed at the site. Transport and handling of the radionuclides will be done in accordance with LLNL, NTS, DOT, DOE, and state regulations.

In the event of power failure an emergency power supply exists at the SFT-Climax facility. In the unlikely event of the failure of the emergency power, the flow system will shut down in a safe manner. There will be no automatic restart capability; instead a remote manual control would be used. The packers are not dependent on the electrical system and will remain in place. The input pumps will cease to function and the pressure will decay. There will be an automatic draining of the central volume. The collection pumps will cease to operate, but gravity will continue to drain the system to the waste storage tank. Unenergized valve positions allow automatic venting to the waste tank where appropriate. Restart decisions, if necessary, will be made by the Project Leader.

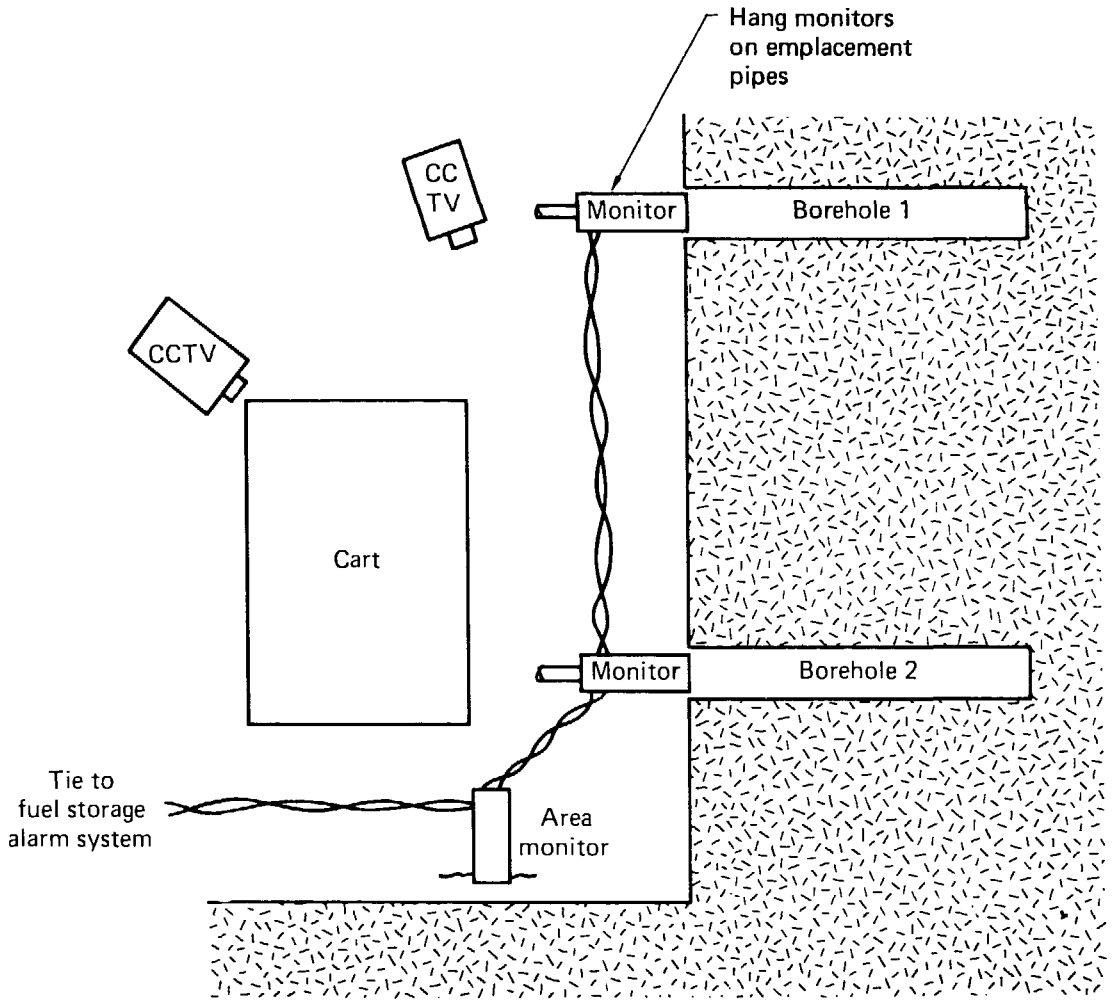

Figure 28. Radiation monitors and closed-circuit TV.

Before radionuclide injection, if the pressurization for the packers should not be operational for any reason, the center volume pump controls will not function and no pressure will be generated. The pressure tap is vented to the waste container, thus relieving pressure in the central volume. Before radionuclide injection, if the water supply for the packers should drop at any time, thus indicating a significant leak, the pumps would be stopped and the central volume vented to waste container. The use of water-tight barricades that fit the open ends of the boreholes appears desirable from the standpoint of radionuclide liquid containment. Emplacement pipe attached to the packer configuration will provide a mechanical barricade.

If after radionuclide injection the packer pressure drops slowly below a preset level and the water-supply load cell indicates a significant leak in the packer pressurization system, the pressure tap valve would vent the central volume to the waste container and the large flow pump would be activated to purge the system (~10 s). What constitutes the preset level or significant leak will be determined by previous testing based on the holding power of the packer vs the applied pressure. If packer pressure failure is sudden, the pressure tap valve would be operated as before but the pump would not be activated to retain as much as possible of the radionuclides. All of these conditions alarm the DACS and area monitoring system. All packer pressurization systems, including packers, will be thoroughly tested prior to installation.

7. QUALITY ASSURANCE

Radiological and industrial safety concerns and the need for obtaining demonstrably valid data necessitate the special control provided by a quality assurance (QA) plan. Such a plan is required of all participants in DOE-NV nuclear waste storage investigations. A QA plan M-078-24 was developed and is being implemented. It was issued by LLNL on September 24, 1980. A Nonconformance Correction Procedure, QP-24-01, has also been issued to serve possible future needs. It is an implementing procedure associated with the QA plan.

This plan and the procedure were developed with the help of the LLNL Quality Assurance Office and with the full participation of the technical project officer, project leader, task leaders, and quality engineer for this project. The plan and procedure use the principles and methodology of the LLNL Quality Assurance Program displayed in the LLNL QA Manual (1978).

The QA plan specifies responsibility assignments and describes required quality control (QC) and QA activities. Covered QC activites include control of samples and test locations, their selection and identification, as well as task planning, support, procedures, test system development and implementation, operations, and documents. Covered QA elements include corrective action, QA records, and QA audit.

8. ACKNOWLEDGMENTS

The authors are grateful to all the reviewers of a draft version of this document for their helpful suggestions and comments. We especially wish to thank Konrad Krauskopf, Peter Sargent, Cliff Davison, and Paul Fenske for their participation in the formal peer review at Las Vegas in March 1982. We also wish to thank Richard Friesen, Jens Mahler, William Russell, Peter Holl, Lyn Ballou, and Sam Spataro for attending the internal design review at LLNL in December 1981. The final version of the ETP has incorporated their suggestions wherever possible. However, as authors of this document we take complete responsibility for the final results.

REFERENCES

Bondietti, E.A., and C.W. Francis, "Geological Migration Potentials of Technetium-99 and Neptunium-237," Sci. 203, 1337 (1979).

Carlson, R.C., W.C. Patrick, D.G. Wilder, W.G. Brough, D.N. Montan, P.E. Harben, L.B. Ballou, and H.C. Heard, SFT-C Technical Measurements Interim Report FY1980, Lawrence Livermore National Laboratory, Livermore, CA, UCRL-53064 (1980).

Failor, R., D. Isherwood, E. Raber, and T. Vandergraaf, Final Report: Laboratory Studies of Radionuclide Transport in Fractured Climax Granite, Lawrence Livermore National Laboratory, Livermore, CA, manuscript in preparation (1982).

Grisak, G.E., J.F. Pickens, and J.A. Cherry, "Solute Transport Through Fractured Media 2. Column Study of Fractured Till," Water Resources Res. 16, No. 4, 731 (1980).

Houser, F.N., and F.G. Poole, Age Relations of the Climax Composite Stock, Nevada Test Site, Nye County, Nevada, USGS Professional Paper 424B, pp. B176-177 (1960).

Holly, D.E., N.L. Guinasso, and E.H. Essington, Hydrodynamic Transport of Radionuclides: One-Dimensional Case with Two-Dimensional Approximation, Teledyne Isotopes, Palo Alto, CA, NVO-1229-179 (1971).

Isherwood, D., et al., Program Plan: Field Radionuclide Migration Studies in Climax Granite, Lawrence Livermore National Laboratory, Livermore, CA, UCID-18838 (1980).

Jacobs, C.E., and S.W. Lohman, "Nonsteady Flow to a Well of Constant Drawdown in an Extensive Aquifer," Trans. Am. Geophys. Union 33, No. 4, 559 (1952).

LLNL Health and Safety Manual, Supplement 32.03, Rev. 12-10-80, "Pressure Vessel and System Design," Lawrence Livermore National Laboratory, Livermore, CA (1980).

LLNL Health and Safety Manual, Section 8, "Hazardous Materials Control," Lawrence Livermore National Laboratory, Livermore, CA (1980).

LLNL Health and Safety Manual, Procedure No. NTS-230, Lawrence Livermore National Laboratory, Livermore, CA (1972).

LLNL QA Manual, Lawrence Livermore National Laboratory, Livermore, CA, M-078, Vol. 1 (1978).

Maldonado, F., Summary of the Geology and Physical Properties of the Climax Stock, Nevada Test Site, U.S.G.S. Open File Report 77-356 (1977).

Morrison, F., Scoping Analysis for Radionuclide Migration Test, Lawrence Livermore National Laboratory, Livermore, CA, UCID-19369 (1982).

Murray, W., Geohydrology of the Climax Stock Granite and Surrounding Rock Formations, Nevada Test Site, Lawrence Livermore National Laboratory, Livermore, CA, UCRL-53138 (1981).

Neretnieks, I., "Diffusion in the Rock Matrix: An Important Factor in Radionuclide Retardation," J. Geophys. Res. 85, No. B8, 4379 (1980).

Raber, E., D. Lord, and P. Burklund, Hydrologic Test System for Fracture Flow Studies in Crystalline Rock, Lawrence Livermore National Laboratory, Livermore, CA (UCID-in press) (1982).

Ramspott, L., et al., Technical Concept for a Test of Geologic Storage of Spent Reactor Fuel in the Climax Granite, Nevada Test Site, Lawrence Livermore National Laboratory, Livermore, CA, UCRL-52796 (1979).

Tang, D.H., E.O. Frind, and E.A. Sudicky, "Contaminant Transport in Fractured Porous Media: Analytical Solution for a Single Fracture," Water Resources Res. 17, No. 3, 555 (1981).

Thorpe, R., and J. Springer, Fracture Mapping for Radionuclide Migration Studies in the Climax Granite, Lawrence Livermore National Laboratory, Livermore, CA, UCID-19081 (1981).

Weed, H., R. Failor, L. Dibley, and I. Murray, An Apparatus for Measurement of Radionuclide Transport Rates in Rock Cores, Lawrence Livermore National Laboratory, Livermore, CA, UCID-19200 (1981).

Wilder, D.G., and W.C. Patrick, Geotechnical Status Report for Test Storage of Spent Reactor Fuel in Climax Granite, Nevada Test Site, Lawrence Livermore National Laboratory, Livermore, CA, UCRL-85096 (1980).

APPENDIX I. EQUIPMENT DESIGN CRITERIA

1. GENERAL SYSTEM REQUIREMENTS

(a) Completely automated system for control of flow rate and maintenance of constant injection pressure to be remotely controlled from mine alcove. Packers to be manually inflated and equipped with pressure-regulator compensation.

(b) Period of service for sample collection, replacement of water supply, and data storage should be once a week with provision for a 7-day grace period.

(c) System tied into DAS on site to provide a fail-safe system with an alarm to notify the operator of malfunctions (i.e., inlet or outlet flow stops, radiation monitor fails, packer pressure fails).

(d) System must be chemically inert and have no sorption capacities for the various radionuclide tracers.

(e) System must be easily transportable (e.g., railcar) with a period of less than 1 week required for move to different location in Piledriver tunnel.

(f) The injection system and sampling packer system will each be a single straddle packer unit that can be manually installed in the drift wall.

(g) The system will meet appropriate industrial and radiation safety standards as required. The experimental design must prepare for concentrated tracer loss or packer leaks. If decontamination is necessary, procedures should be fairly easy.

(h) Be equipped with either a separate data acquisition system (DAS) independent of SFT computers or the capabilities to interface with SFT computers at a reasonable cost.

(i) If power outage at Climax outlasts auxiliary power supply, system will safely shut down; however, packers will remain in place.

(j) Monitoring by closed-circuit TV from the DAS trailer will be possible.

(k) A stop switch will be located on the surface and in the drift to shut down the experiment if necessary. However, packers will remain inflated.

(l) No upgrade of utilities in mine drift is anticipated.

2. INJECTION SYSTEM

(a) Packer system that allows isolation of a designated fracture(s)in which constant pressure is maintained in packers to ensure a continuous seal.

(b) Packers to be Cobbs type, inflated by gas over hydraulics.

(c) Water injection pressure 0 to 100 psi with flow rate 0.25 to 6.0 ml/min (higher flow rates are possible with backup pump of 1.5 to 30.0 ml/min).

(d) Injection pressure in interval between packers must be controlled, automatically monitored, and recorded to $\pm$1% variation.

(e) Inlet system must be capable of injecting a radionuclide solution whether as a single concentrated pulse (5 to 10 ml) or as a continuous injection into an existing flow field. This system must allow subsequent tracers to be injected without contamination or dilution problems. We will expect a 10:1 input dilution of tracer.

(f) Time must be recorded using some type of event markers (i.e., ΔP). The time the tracer enters the borehole must be accurately known.

(g) Water must be ultrafiltered ($<0.01\ \mu m$) before entering the borehole. The water-tank capacity necessary to fit a 14-day automated period is estimated as a 50-gal tank with a 50-gal auxiliary tank.

(h) Constant injection pressure is essential. (We are assuming constant flow rate will occur after steady-state conditions are reached.) The capability of constant injection flow rate would be nice, but is not essential. However, flow rate must be monitored and recorded.

3. COLLECTION SYSTEM

(a) Must be able to remove samples periodically, by-passing collector (i.e., going into waste mode) to make simple analytical measurements (i.e., Eh, pH, ΔT).

(b) Samplers must be able to accommodate a maximum of 750 samples with sampling size flexible to 10 to 50 ml with a maximum sampling rate of 1/min.

(c) Samples must be collected automatically during the test period with all sampling rate changes done manually. The sampling system will be tied into the DAS such that if a sample volume exceeds a certain value, the sampler will automatically advance to the next sample vial.

(d) Each sample vial and holder will be coded and marked such that the DAS will automatically record sample number, time, Δt, and date every time the sampler advances. If the sampler is manually set to go to waste discard, the DAS system will automatically record the time this occurs and the time it ends.

(e) Contamination of dilute tracer samples coming from the outlet hole must be avoided (e.g., evaporation, dust, sorption by sample container or tubing).

(f) Collection of samples to be time dependent. Sample size can be approximate.

(g) Volume of fluid in collection interval should be kept to a minimum (<12 ml), with as slowly a varying output flow rate as possible. This is to ensure the maximum time resolution.

4. REQUIREMENTS FOR ON-LINE SENSORS

(a) On-line detectors measuring β^- and γ, each with a multichannel analyzer (MCA). The MCA will sum the data from each channel to obtain a single value in each region of integration. The MCA has a threshold detection limit.

(b) A flow-through sample arrangement with throw-away flow-through tubes that eliminate cross contamination from experiment to experiment.

(c) A high efficiency unit that can detect low levels of activity.

(d) Rugged: able to withstand conditions (humidity); require little or no routine maintenance; and stable over expected temperature range.

(e) Choice of output with a selection of total integrated activity or activity of separate nuclides.

(f) DAS-compatible output/control system.

(g) The system will be capable of continuous flow counting.

(h) The MCA will have cathode-ray tubes (CRTs) to visually display the spectrum as data are being collected.

5. DATA ACQUISITION SYSTEM (DAS)

(a) No computational or graphic power is necessary (some simple computations would be useful).

(b) Collection of two types of data from on-line sensors: (1) integrated areas around each peak of interest and (2) the full spectrum, channel by channel. This will be a maximum of 24 points from the MCAs plus 2 points for the time the spectra were taken.

(c) In addition to the DAS, a paper tape printer is necessary to record the output of each region of integration. This should always be accessible. We do not need a separate display of the full spectra.

(d) Periodically record the full spectrum from each MCA. This will be 1026 data points [one point/channel (1024 channels) and the time and duration of the count for each spectrum]. This is a total of 2052 data points.

(e) Record the integrated data (ROIs) every 5 to 10 min. The full spectra are to be recorded every hour.

(f) Data can be put onto either magnetic tapes or discs.

APPENDIX II. SPECIFIC EQUIPMENT LIST

1. PACKER SYSTEM

Gas bottles
Fittings
Regulators
Pressure vessels
Valves
Check valves
Pressure gauges
Pressure transducers
Tubing--SS
Viton packer seals
Emplacement pipe
Containment bags

2. INJECTION SYSTEM

Reservoir
Filter pump
Filter
Check valves
Bypass valves
Valve actuators and solenoid
Pumps
Tubing--SS
Tubing--Teflon
Fittings
Viton coating
Pressure transducers

3. COLLECTION SYSTEM

Waste tank
Viton coating
Level sensor
Pumps
Tubing--Teflon
Fittings
Valves
Check valves
Bypass valves
Valve actuators and solenoids
β^- detector (Radiometer Instruments and Chemicals, Inc. Flow-One 4P)
γ detector NaI(Tl) crystal and accessories
Samplers (Gilson Escargot)
Pressure transducers

4. DATA ACQUISITION AND CONTROL SYSTEM

Multichannel analyzer
LSI-11 microprocessor
Incremental scanners
TV monitor
Magnetic tape
Programmable sequencer
Proximity detector
Bar-code reader
LSI 11/23 microprocessor
HP 1000

5. PHYSICAL SYSTEM

Hydraulic cart
Control system cart
Water and waste tank cart
Radiation monitors

U.S. Government Printing Office: 1982/7-587-002/4073